Chapter 7.0

Roof support design methodology

7.1 Introduction

In order to develop an engineering design, it is essential to understand the roof and support behaviour and the interaction between them. A detailed analysis of the data given in the previous Chapters was therefore conducted and the results are presented in this Chapter.

As demonstrated in the previous Chapters that in an underground environment rock and support properties and performances can vary significantly within a short distance. The roof stability is strongly dependent on these varying properties of roof-support system. These properties can be described using deterministic and/or probabilistic models. Deterministic models typically use a single discrete descriptor for the parameter of interest. Probabilistic models however describe parameters by using discrete statistical descriptors or probability distribution (density) functions. Therefore, a roof support design methodology based on probabilistic approach has been developed and presented in this Chapter. It is considered that for real world roof support problems, the values of input parameters are not constant and a single safety factor cannot be used.

It is however not intended to present a complete and rigorous treatment of the fundamentals of probabilistic design approach, therefore the formal theory of probability is summarised and a functional description is presented.

7.2 Support design based on a probabilistic approach

In traditional deterministic (calculation of a single safety factor) roof bolt design methodologies, the input parameters are represented using single values. These *certain* values are described typically either as “best guess” or “worse case” values. However, investigations into the roof and roof bolt behaviour presented throughout this thesis suggest that the input parameters, including the mining geometries, rock and support properties can vary significantly within a few meters in a panel and also from one support product to another. This is the fundamental principal of probabilistic design approach, which is the recognition of that these factors which govern the roof stability and support performance exhibit some degree of natural uncertainty. Ideally, this uncertainty should be accounted for in the design method. While deterministic approaches provide some insight into the underlying mechanisms, they are not well-suited to making

predictions to roof support decision-making, as they cannot quantitatively address the risks and uncertainties that are inherently present. In a probabilistic design method however, the stochastic nature of the input parameters are included and therefore, it is possible to quantitatively represent uncertainties thus the resulting probability of failures. Dealing with probabilities of failure rather than safety factors means that it is acknowledged that realistically there is always a finite chance of failure, although it can be very small.

7.2.1 Rules of probability

The first rule of probabilistic approach is that, by convention, all probabilities are numbers between 0 and 1. A probability of 0 indicates an impossible event, and a probability of 1 indicates an event certain to happen. Most events of interest have probabilities that fall between these extremes.

The second rule states that, if two events are dependent (i.e., knowing the outcome of one provides information concerning that the other will occur), then the probability that both events will occur is given by the product of their combined probabilities. Assume, E_1 and E_2 are two events and the event that both E_1 and E_2 occur is described as $P[E_1E_2]$ and is calculated:

$$P[E_1E_2] = P[E_1]xP[E_2 / E_1] \quad [7\text{-}1]$$

where $P[E_2/E_1]$ is the probability of E_2 occurring given that E_1 has taken place. If E_1 and E_2 are independent, that is the occurrence of one does not affect the probability of occurrence of the other, indicating that the probability of two independent events occurring is the product of their individual probabilities:

$$P[E_2 / E_1] = P[E_2] \quad [7\text{-}2]$$

$$P[E_1E_2] = P[E_1]xP[E_2] \quad [7\text{-}3]$$

Probabilistic methods have long been used mainly in civil and other engineering disciplines. Examples of this can be found where probabilistic design methods are used almost routinely to assess the failure probability of building structures and rock slopes.

7.2.2 Methodology of probabilistic approach

The general methodology of probabilistic approach assumes that the load (L) and the strength (S) of a structure can be described by two probability density functions, respectively, as shown in Figure 7-1. The respective mean and standard deviations of each distribution is denoted m_S and s_s for the strength, and m_L and s_L for the load. From Figure 7-1 it can be seen that the two curves overlap meaning that there exist values of strength which are lower than the load, thus

implying that failure is possible in this overlap area. In a purely deterministic approach using only the mean strength and load, the resulting factor of safety would have been significantly larger than unity which implies stable conditions.

To be able to calculate the probability that the load exceeds the strength of a construction element, it is common in Civil Engineering to define a safety margin, SM, as

$$SM = S - L \qquad [7\text{-}4]$$

The safety margin is one type of performance function which is used to determine the probability of failure. The performance function is often denoted $G(X)$, hence:

$$G(X) = S(X) - L(X) \qquad [7\text{-}5]$$

where X is the collection of random input parameters which make up the strength and the load distribution, respectively. An alternative formulation of the performance function which is often used in geomechanics involves the factor of safety, F_S. Failure occurs when F_S is less than unity, hence the performance function is defined as:

$$G(X) = F_S - 1 \qquad [7\text{-}6]$$

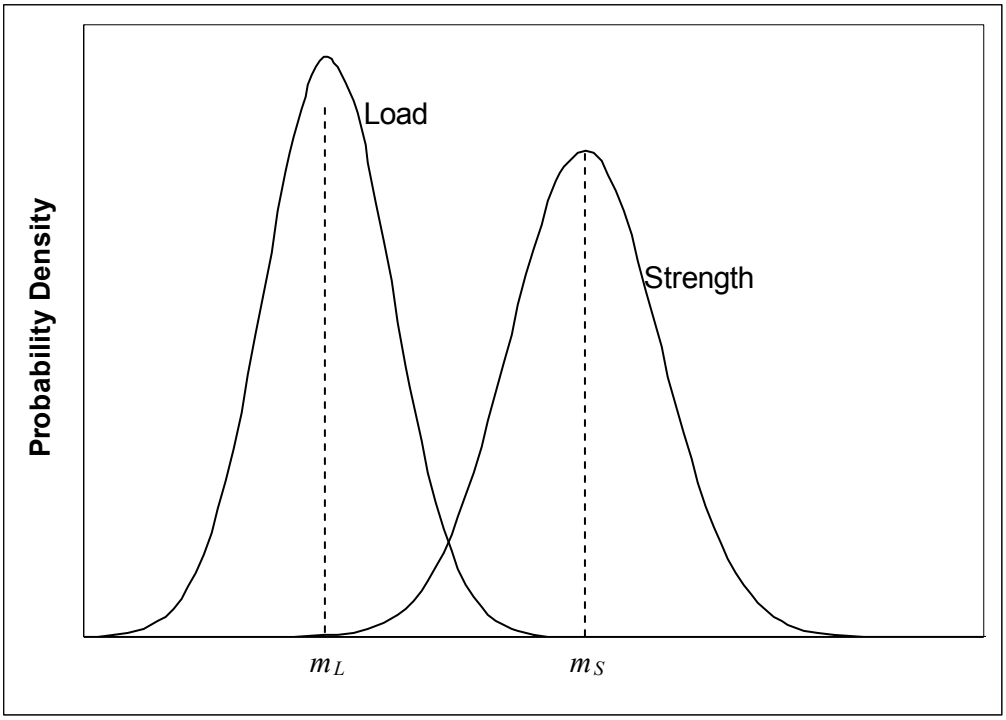

Figure 7-1 Hypothetical distribution of the strength and the load

The probability density function (PDF) for the safety margin is illustrated in Figure 7-2. This Figure indicates that failure occurs when the safety margin is less than zero. The probability of failure (PoF) is the area under the density function curve for values less than zero, as shown in

Figure 7-2. The reliability of a structure, on the other hand, is defined as the probability that the construction will *not* fail. The same concept applies to any performance function.

Assuming that the performance function can be expressed according to either Equation [7-5] or [7-6] and that the strength and load distributions can be defined, using a 3-level analysis (Level 1, Level 2 and Level 3), probability of failure can be calculated. A Level 1 analysis is basically a deterministic analysis, i.e. only one parameter value is used for every variable. In a Level 2 analysis, each stochastic variable is characterized by two parameters, the mean and the standard deviation, as described above. A Level 3 analysis is the most complete and sophisticated method of assessing the probability since the exact statistical characteristics of all variables are taken into account and the joint probability density functions are calculated. Level 3 analysis is fairly uncommon since it often is very difficult to describe and quantify the "joint probability density functions" (Mostyn and Li, 1993).

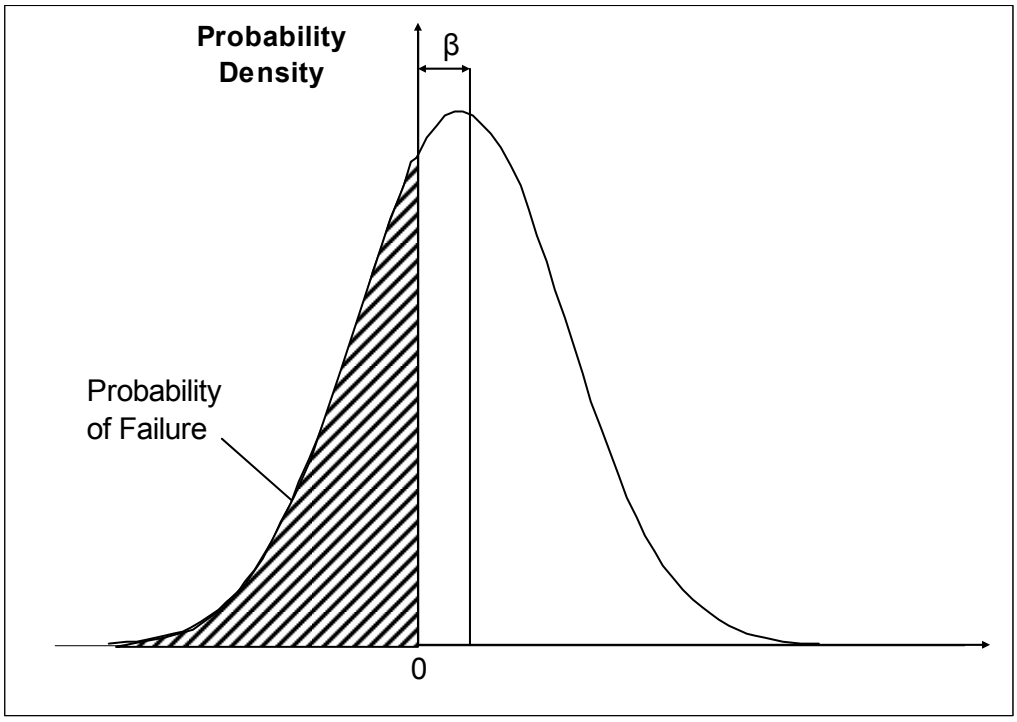

Figure 7-2 Hypothetical distribution of the safety margin, SM.

In practical Civil Engineering design, Level 2 analysis is most commonly used and found acceptable (Sjoberg, 1996). Level 2 analysis is also adopted in this thesis. In this approach, the probability of failure is evaluated using a reliability index, β, defined in terms of the mean and the standard deviation of the trial factor of safety:

$$\beta = \frac{m_G - 1}{s_G} \qquad [7\text{-}7]$$

where m_G and s_G are the mean and standard deviation of the performance function, respectively. The reliability index (RI) is thus a measure of the number of standard deviations separating the mean factor of safety from its defined failure value of 1.0, Figure 7-2. It can also be considered as a way of normalising the factor of safety with respect to its uncertainty. When the shape of the probability distribution is known, the reliability index can be related directly to the probability of failure. In Civil Engineering, especially in building construction design, the reliability index has been linked to safety classes for buildings. This will be discussed in detail further in this Chapter.

Exact solutions for calculating the failure probability is only possible for simple cases. The performance function contains several variables describing the load and strength and is therefore often non-linear, which prohibits exact analytical solutions. A commonly used approximate method is the first-order-second-moment method (FOSM) in which the performance function is approximated by a polynomial expansion into a linear expression. Using a linear expression, the mean and standard deviation of the performance function and also the reliability index can be calculated using standard statistical formulae (Mostyn and Li, 1993). The resulting distribution of the performance function can be assumed to be a normal distribution, according to the central limit theorem (Kreyszig, 1988). Consequently, the resulting failure probability can be calculated as $\Phi(-\beta)$ where Φ is the standardised normal distribution which can be found tabulated (Kreyszig, 1988). The FOSM provides no information about the shape of the probability density function. To estimate any probability, the shape of the probability distribution of the output has to be assumed. This assumption of, typically, a normal or a lognormal distribution introduces a source of inaccuracy.

An alternative technique is the point estimate method (PEM), which is based on the precept that a probability distribution can be represented by point estimates. In this method the performance function is evaluated 2^N times (N being the number of input variables) to obtain the mean and standard deviation of the performance function (Rosenblueth, 1975). This method is very simple for two-three variables and does not require extensive mathematical derivations, however, become impractical for large numbers of input parameters.

Another slightly different definition of the reliability index is that given by Hasofer and Lind (1974), in which the reliability index is defined as the shortest distance from the origin and to the boundary of the limit state. The function is the limit state is determined from the performance function by transforming to statistically uncorrelated variables. The reliability index β can then be determined iteratively. Hasofer-Lind's (1974) method is common in building construction design but has limitations regarding how complex the performance function can be to do the transformation to uncorrelated parameter space.

All of the above methods are analytical means of determining the reliability index from a number of stochastic variables which make up the performance function. In cases where the performance function is complex and contains a large number of variables, a simulation technique can instead be used. The most common simulation technique is the Monte Carlo method. In this method, the distribution functions of each stochastic variable must be known. From each distribution, a parameter value is sampled randomly and the value of the performance function calculated for each set of random samples. If this is repeated a large number of times, a distribution of the performance function is obtained. The probability of failure can be calculated as the ratio between the number of cases which failed and the total number of simulations. Alternatively, the mean and standard deviation of the performance function distribution (factor of safety) can be calculated to yield the reliability index from which the failure probability can be determined using tabulated values for the standardised normal distribution (Kim et al. (1978); Mostyn and Li (1993)).

Monte Carlo simulation is thus a procedure in which a deterministic problem is solved a large number of times to build a statistical distribution. It is simple and can be applied to almost any problem and there is practically no restriction to the type of distribution for the input variables. The drawback is that it can require substantial computer time. This becomes especially important when relatively small probabilities are expected and hence many iterations are required to obtain a reliable measure of the tails of the distribution. To overcome this, more efficient Latin Hypercube sampling technique has been developed. In this method, stratified sampling is used to ensure that samples are obtained from the entire distribution of each input variable. This results in much fewer samples to produce the distribution of the performance function, in particular for the tails of the distribution (Nathanail and Rosenbaum, 1991; Pine, 1992). With today's powerful computers and widely available softwares, such as RiskAMP (utilised in this thesis) and @RISK, computational time has become less of a problem and Monte Carlo methods prevail as the most common simulation techniques.

In general, the implementation of Monte Carlo method involves:

- Selection of a model that will produce a deterministic solution to a problem of interest.
- Decisions regarding which input parameters are to be modelled probabilistically and the representation of their variabilities in terms of probability distributions.
- Repeated estimation of input parameters that fit the appropriate probability distributions and are consistent with the known or estimated correlation between input parameters.
- Repeated determination of output using the deterministic model.
- Determination of the probability density function of the computed output.

As mentioned above, the fundamental to the Monte Carlo method is the process of explicitly representing the uncertainties by specifying inputs as probability distributions. By describing the process as a probability distribution, which has its origins in experimental/measurement *continuous* data, an outcome can be sampled from the probability distributions, simulating the actual physical process/measurement.

This process requires a collection of actual measurements and determining the best fits to the data using the goodness of fit tests (GOF). GOF tests measure the compatibility of a random sample with a theoretical probability distribution function. Three most common GOF tests are:

- Kolmogorov-Smirnov
- Anderson-Darling
- Chi-Squared

The details of the probability distributions, GOF tests and random selection of design parameters are given in Section 7.6.

7.2.3 Required number of runs in Monte Carlo simulation

Probabilistic analysis using the Monte Carlo simulation involves many trial runs. The more trial runs used in an analysis, the more accurate the statistics will be. The number of required Monte Carlo trials is dependent on the desired level of confidence in the solution as well as the number of variables being considered (Harr, 1987), and can be estimated from:

$$N_{mc} = \left[\frac{d^2}{4(1-\varepsilon)^2} \right]^m \qquad [7\text{-}8]$$

where N_{mc} = number of Monte Carlo trials, d = the standard normal deviate corresponding to the level of confidence, ε = the desired level of confidence (0 to 100%) expressed in decimal form; and m = number of variables.

The number of Monte Carlo trials increases geometrically with the level of confidence and the number of variables. For example, if the desired level of confidence is 90%, the normal standard deviate will be 2.71, the number of Monte Carlo trials will be 68 for one variable, 4,575 for two variables, and 309,445 for three variables. Theoretically, for a 100% level of confidence, an infinite number of trials would be required.

For practical purposes, the number of Monte Carlo trials is usually in the order of thousands. This may not correspond to a high level of confidence when multiple variables are being considered; however, the statistics computed from the Monte Carlo simulations are typically not very sensitive to the number of trials after a few thousands trials (Allen et al., 2002).

7.2.4 Acceptable probability of stability

Another important consideration in using the probabilistic approach is to use an *acceptable* PoF in the design.

Vrijling and van Gelder (1998) defined the following three kinds of limit states to construct a breakwater and recommended probability of failures depending on the failure characteristics:

i) Ultimate Limit States (ULS), describing immediate collapse of the structure.
ii) Serviceability Limit States (SLS), describing loss of function of the structure without collapse
iii) Accidental Limit States (ALS), describing failure under accident conditions (collision, explosions).

Vrijling and van Gelder (1998) stated that usually low PoF required for ULS compared to SLS and ALS in which the effects of failure are easily reversed.

Vrijling and van Gelder (1998) developed the following classification and Table 7-1 to be used in the design of vertical breakwaters considering the probability of loss of life due to failure of the structure:

- Very low safety class, where failures implies no risk to human injury and very small environmental and economic consequences.
- Low safety class, where failures implies no risk to human injury and some environmental and economic consequences.
- Normal safety class, where failures implies risk to human injury and significant environmental pollution and high economic or political consequences.
- High safety class, where failures implies risk to human injury and extensive environmental pollution and high economic or political consequences.

Table 7-1 Acceptance probability of failures for different safety class (after Vrijling and van Gelder, 1998)

Limit State Type	Design Probability of Failure			
	Very Low	Low	Normal	High
SLS / ALS	40%	20%	10%	5%
ULS	20%	10%	5%	1%

Form the above Table it is evident that even in ultimate limit state 10 to 5 per cent probability is acceptable for low to normal safety classes.

The probabilities used in the design of open cast slopes are discussed with Priest and Brown (1983) and Pine (1992), who defined acceptance criteria according to Table 7-2.

This Table indicates that for benches, probability of failure of around 10 per cent is accepted, whereas for an overall slope, a failure probability of less than 1 per cent would be more suitable.

Table 7-2 Acceptance criteria for rock slopes (after Priest and Brown, 1983; Pine, 1992)

Category and Consequences of failure	Example	Reliability Index (β)	Probability of Failure
1. Not serious	Non-critical benches	1.4	10%
2. Moderately serious	Semi-permanent slopes	2.3	1 – 2 %
3. Very Serious	High/permanent slopes	3.2	0.3%

A design criteria based on probability of failure is also recommended for Western Australian open cast mines, Table 7-3. These design criteria have been developed from a combination of DME assessment of open cast mines in Western Australia and a selection of published literature.

Similarly, this Table suggests a probability of failure of 1 per cent as acceptable in serious slopes. This decreases to 0.3 per cent in populated areas where the slopes are near public infrastructures.

Based on these previous experiences, the probabilistic design criteria presented in Table 7-4 is tentatively suggested for roof bolting system design. It is however recommended that this design criteria should be evaluated before fully implemented in underground coal operations.

Table 7-3 Examples of design criteria for open pit walls (after DME, 1999)

Wall class	Consequence of Failure	Design Probability of Failure	Pit wall examples
1	Not Serious	Not applicable	Walls (not carrying major infrastructure) where all potential failures can be contained within containment structures.
2	Moderately Serious	10%	Walls not carrying major infrastructure.
3	Serious	1%	Walls carrying major mine infrastructure (e.g. treatment plant, ROM pad, tailings structures).
4	Very Serious++	0.30%	Permanent pit walls near public infrastructure and adjoining leases.

\+ Potential failures have been defined as those modes of pit wall failure that have a POF of greater than 10%.
++ Where a mutually acceptable agreement to allow mining cannot be made between the mining company and the "owner" of the adjoining structure or plot of land. Note that a higher standard of geotechnical data is required for the design of category 3 and 4 slopes compared to category 1 and 2 slopes.

Table 7-4 Suggested design criteria for the roof bolting systems

Roof class	Risk Category	Reliability index (β)	Design Probability of Failure	Example
1	Moderately Serious	1.4	5%	Short term requirement (< 1 year), personnel access partially restricted
2	Serious	2.3	1%	Medium term requirement (1 - 5 years) personnel access partially restricted
3	Very Serious	3.2	0.3%	Long term requirement (> 5 years) no personnel access restrictions

In Civil Engineering, probabilistic design has advanced to the stage that virtually all building regulations are based on a probabilistic approach. The development has not yet reached this point in the field of geomechanics. One of the reasons for this is the difficulty associated with describing a rock mass quantitatively and defining a model which describes both the strength and the load acting on rock. This requires knowledge of roof failure mechanisms and a model which describes how failure occurs. The following sections of this Chapter aim at developing a deterministic model of failure mechanisms and a load/strength relationship to be used to develop a probabilistic design methodology for coal mine roof support design.

7.3 Roof behaviour and failure mechanism

In order to develop a realistic roof behaviour model, data presented in Chapters 3 and 4 was analysed in detail. A total of 55 intersection and roadway measurements from depths of 32 m to 170 m situated in significantly different geotechnical environments were analysed in terms of height and magnitude of instabilities in the roof. The aim of this analysis was to:

1. establish at what heights the instabilities took place,
2. how these instabilities can be supported, and
3. establish a roof behaviour based on the magnitudes of deformations.

The results obtained from the height of instabilities are presented in Figure 7-3. This figure shows that the maximum measured height of instabilities in South African collieries is limited to 2.5 m into the roof, and there is no evidence of a substantial increase in the height of instabilities, as is the case in some overseas coal mines, Figure 7-4.

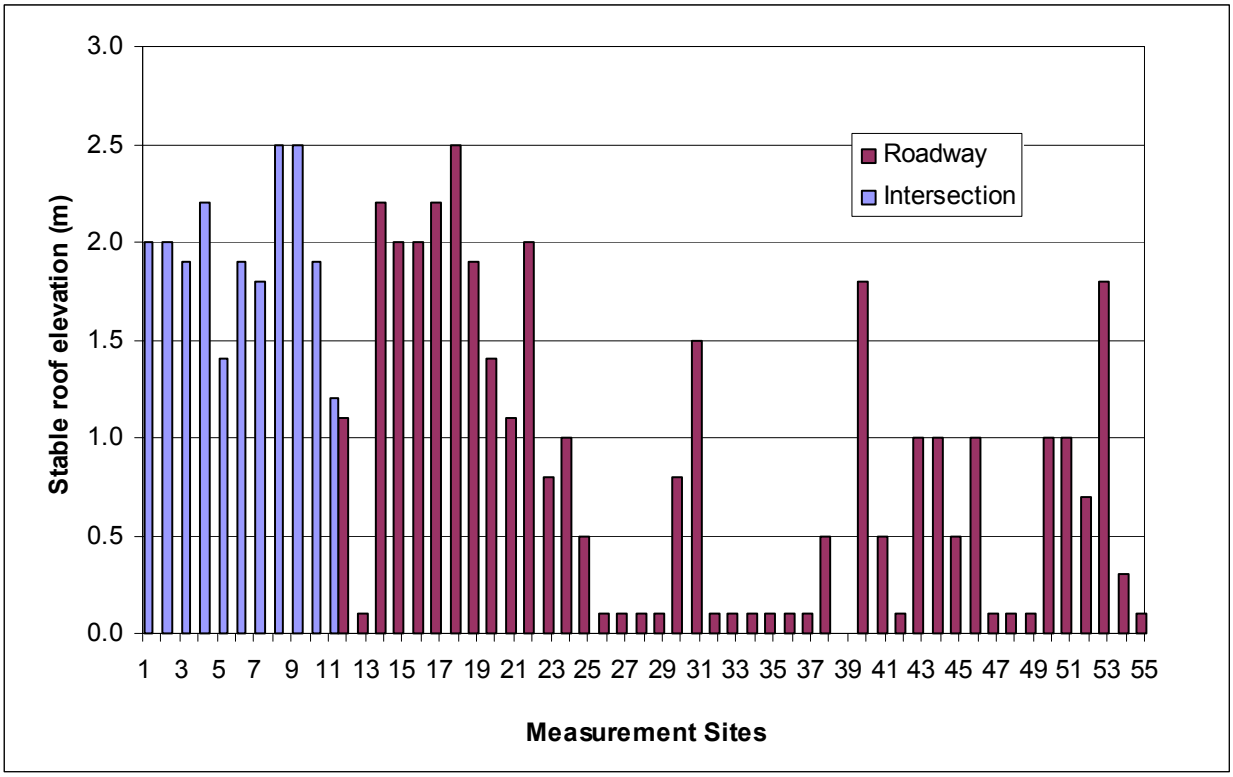

Figure 7-3 Measured height of roof-softening in intersections and roadways in South African collieries

Figure 7-4 An example of roof-softening in a coal mine in the USA (courtesy of Dr. C. Mark)

The height of instability measurements are also compared against the investigations conducted on falls of ground fatalities for the period 1970 to 2003 by Vervoort (1990) and as part of this thesis.

Vervoort (1990) investigated the falls of ground fatalities in South African collieries for the period 1970-1988. A similar study has also been conducted as part of this thesis covering the period 1989 to 2003. Figure 7-5 compares the two data sets with respect to thickness of fall. This Figure indicates that, for 33 year period, a large proportion of fall of ground accidents was due to relatively small falls of ground. However, the proportion of larger falls of ground has increased slightly in the recent data.

The cumulative distribution of thicknesses which caused FOG fatalities during the period 1989 to 2003 and the roof-fracturing heights measured underground are shown in Figure 7-6.

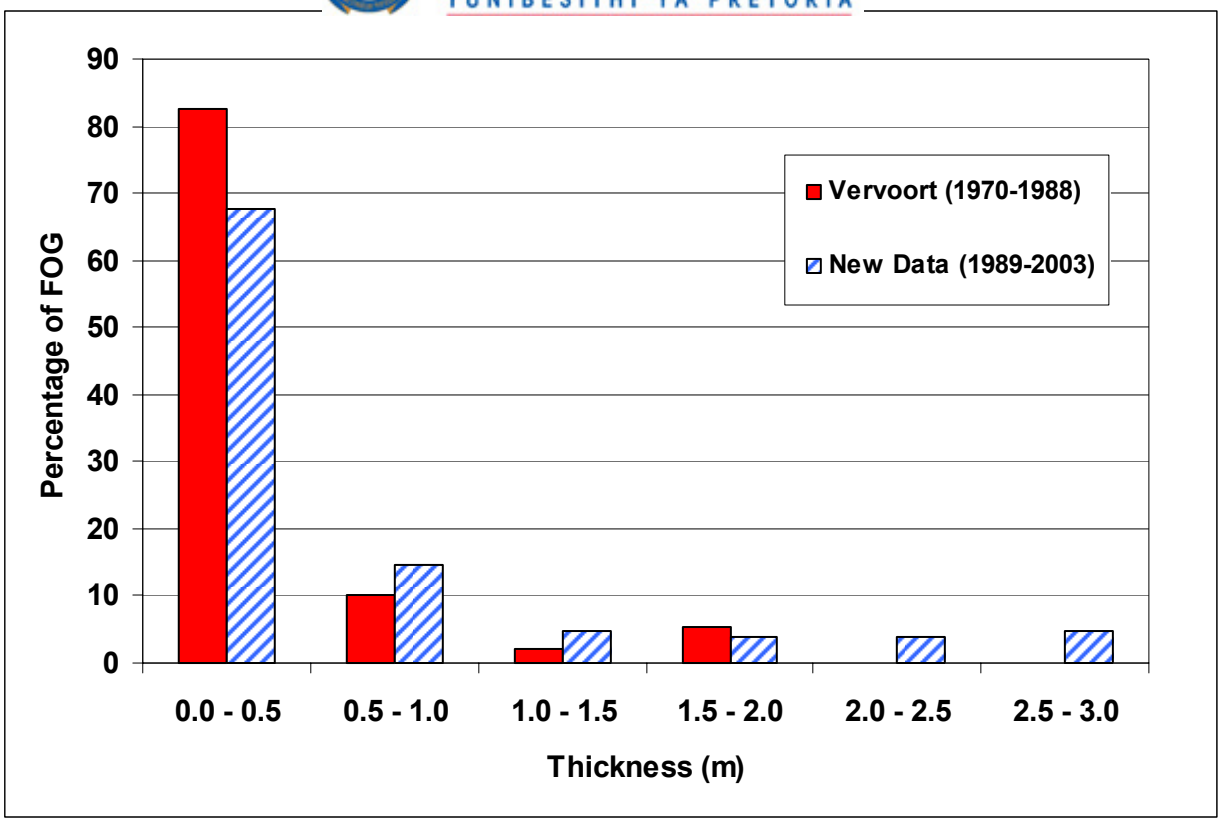

Figure 7-5 The vertical dimension (thickness) of FOG causing fatalities for the period 1970 – 1995

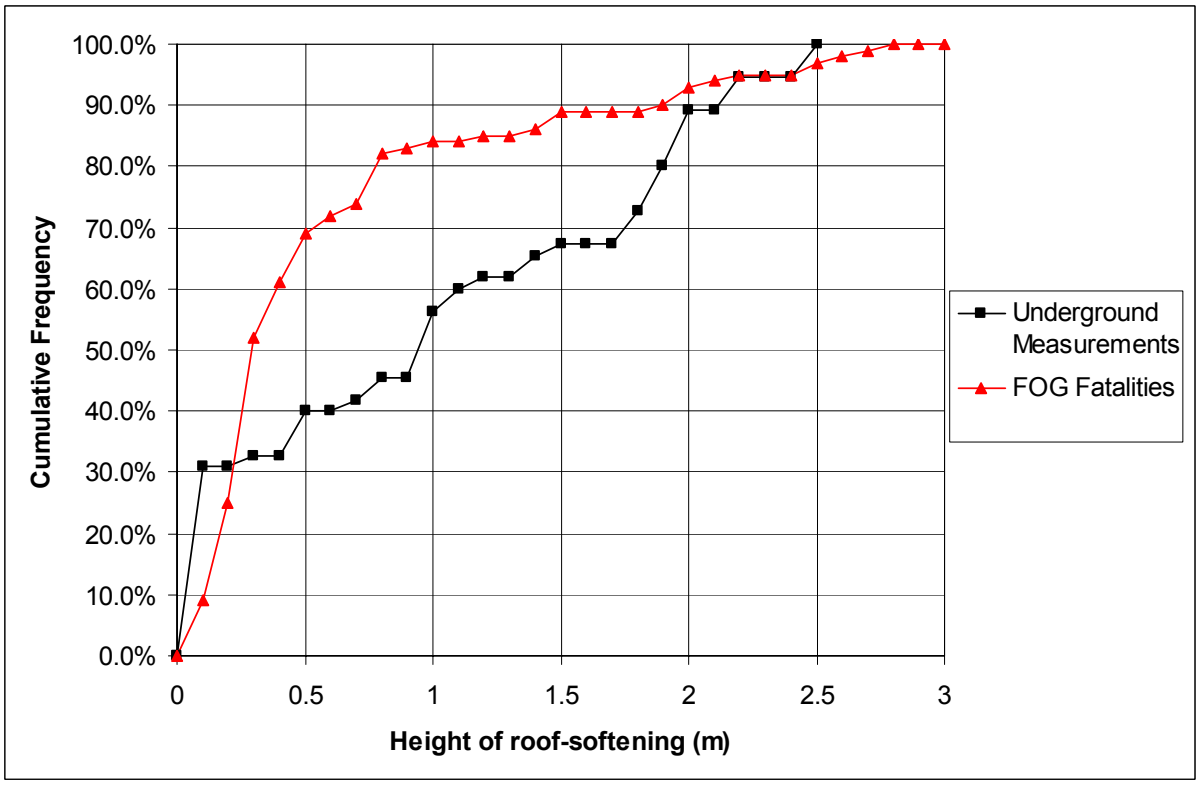

Figure 7-6 Cumulative distribution of FOG thicknesses and the height of roof softening measured underground

Using the underground measurement data, a comparison was also made between the magnitude of deformations in intersections and roadways. The results indicated that, for a 41 per cent increase in the span (taken across the diagonal of an intersection) relative to the roadway span, the magnitude of the displacement in the roof increased by a factor of about four on average, Figure 7-7.

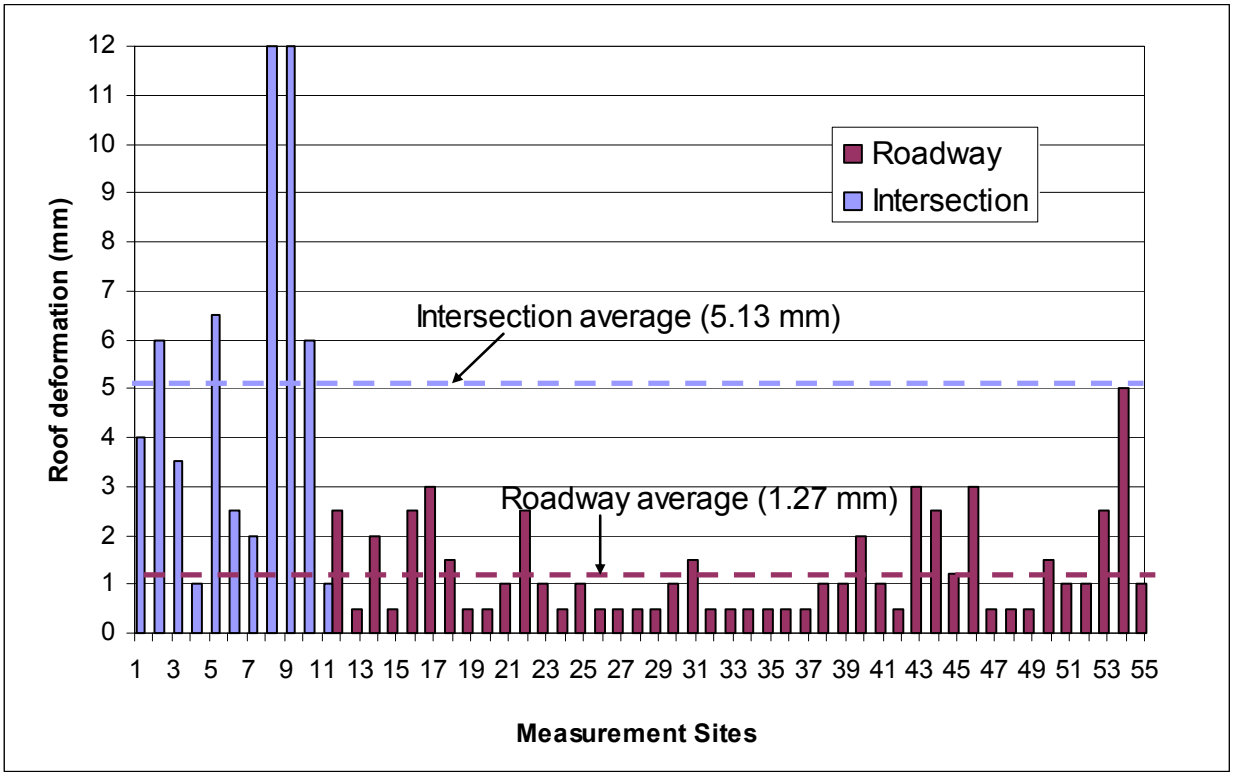

Figure 7-7 Measured deformations in intersections and roadways

The magnitude of measured deformations is also evaluated against the maximum theoretical deflection in a built-in beam using the following formula:

$$\eta_{\max} = \frac{\rho g L^4}{32 E t^2} \qquad [7\text{-}9]$$

where L = roof span (width of roadway)

t = thickness of roof layer (m)

ρ = density of suspended strata (kg/m^3)

g = gravitational acceleration (m/sec^2)

E = Elastic modulus (Pa)

If the roof span (L) in the above formula increases by 41 per cent due to the diagonal width of the intersections, the deformation increases by a factor of 4.0. This is in accord with the findings in Figure 7-7.

The results obtained from the magnitudes of deformations in intersections and roadways reveal that there is a significant correlation between the underground measurements and the beam theory. Also, in the light of the similar correlations found in other Chapters, it is therefore concluded that the roof behaviour in South African collieries can be classified as similar to that of a clamped beam.

The results also suggest that based on the height of softening measurements and the fall of ground fatality data collected over for 33 years, the suspension and beam building mechanisms (with improvements as discussed further in this Chapter) that have been used in South African collieries for many years are, in general, applicable where the appropriate conditions exist. It is however essential to determine the correct support mechanism to ensure the stability of roof.

From the results presented above, the roof behaviour model presented in Figure 7-8 is suggested.

This model suggests that when an underground opening is made, the portion of the strata directly above the opening loses its original support and the stress equilibrium is disturbed. The roof starts to sag under the gravitational and/or horizontal forces (irrespectively) up to a height where there is a competent layer and a new equilibrium is reached. In the case of absence of competent layers, as the lower layers start losing their integrity, the height of instabilities increase further into the roof. To maintain the stability, it is essential to keep the immediate, softened zone stable (Figure 7-8) using either suspension or the beam building mechanism. In beam building mechanism, roof bolts in this zone force all the bolted layers to sag with the same magnitude; the layers within the bolting range thus act like a solid beam supporting the bolted horizon as well as the surcharge load due to softened layers higher into the roof.

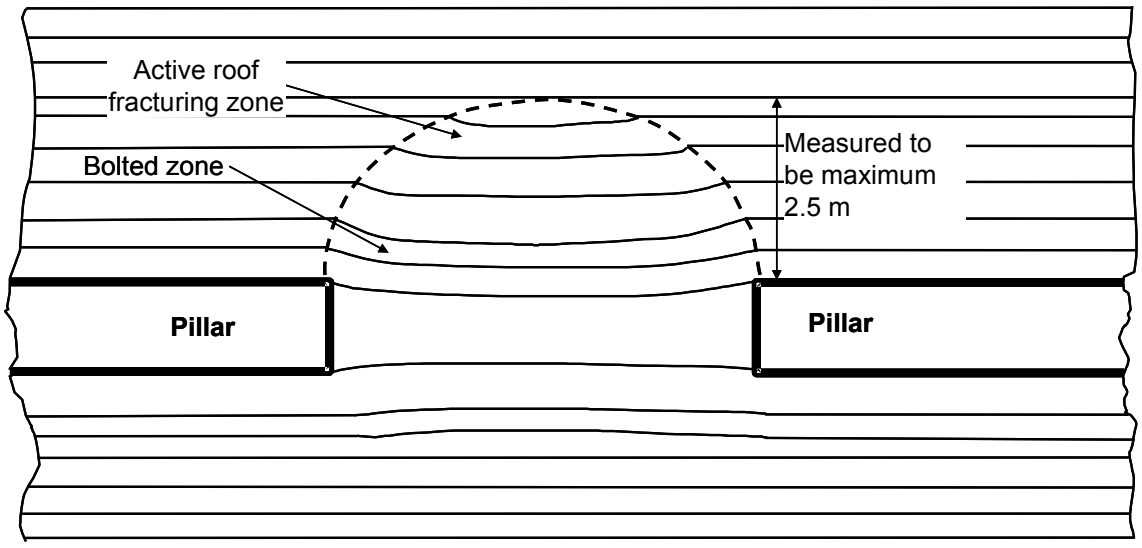

Figure 7-8 Zone of roof softening

7.3.1 Failure and support mechanisms

As indicated in the above model, before a roof bolt system is designed for a certain support mechanism, it is important to establish the geology for at least 2.5 m into the roof (based on measurements), which will assist in identifying the expected roof behaviour and in determining the support mechanism to be used.

If the immediate roof is very weak, but a competent layer exits higher in the roof, the suspension support mechanism is indicated. However, when the entire roof consists of a succession of thin beams, none of which are self-supporting, the suspension principle cannot be applied in this case beam building mechanism is suggested.

It is suggested that before any decision has been made regarding the support system, a detailed geotechnical investigation should be conducted (especially in greenfield studies) to determine the heights of roof softening, which can be assumed to be extended up to the “poor” quality layers. This investigation can be carried out using the standard laboratory tests, impact splitting tests, RQD or Rock Mass Rating.

In the suspension mechanism, the lower (loose) layer is suspended from the upper (competent) layer using roof bolts (van der Merwe and Madden, 2002), Figure 2-12. This creates a surcharge load and increases the maximum tensile stress in the upper layer, above the abutments. This surcharged tensile stress ($\sigma_{xx(\max)}$ in Pa) can be calculated using the following formula;

$$\sigma_{xx(\max)} = \frac{\rho g (t_{com} + t_{lam}) L^2}{2 t_{com}^2} \qquad [7\text{-}10]$$

where, ρ = density of suspended strata (kg/m^3)
g = gravitational acceleration (m/s^2)
L = span (bord width or intersectional diagonal width) (m)
t_{com} = competent layer thickness (m)
t_{lam} = laminated lower strata thickness (m)

For stability to take place, the tensile strength of the competent layer should be greater than the tensile stress generated in this layer due to surcharge load.

It should be noted that as mentioned above, the thickness of competent layer, the position of competent layer, the bord widths, the thickness of suspended strata and the strength of competent layer will vary in nature. It is therefore suggested in determination of the applicability

of the suspension mechanism using Equation [7-10] that a minimum of probability of stability of (PoS) 99 per cent should be attained.

Regarding the tensile strength of rock mentioned above, it should be noted that the tensile strength of rock is determined by the resistance of rock to tension. The failure of rock under tension is invariably abrupt with total loss of cohesion and load carrying ability. Direct determination of tensile strength for rock, i.e. “pull tests”, is difficult, mainly because of involved specimen preparation. Indirect methods are most commonly used for determining the tensile strength.

The Brazilian (disc) method has proven to be a useful technique for a wide range of rock materials. It has, however, been found that the tensile strength determined by Brazilian tests is usually higher than the direct pull test value.

In general, while a rock material may have a tensile strength, a rock mass is often assumed to have very low tensile strength. This assumption is considered appropriate given the existence of joints and other defects in the rock mass. It is suggested that a detailed analysis should be conducted in determining the tensile strength of coal measure rock.

7.4 Roof bolting mechanisms

7.4.1 Suspension mechanism

As mentioned in Chapter 2.0, suspension mechanism (Figure 2-12) is the most easily understood roof bolting mechanism. While the majority of roof bolts used are resin point anchors, mechanical anchors are also uncommonly used (2 per cent only, Henson, 2005).

The design of roof bolt systems based on the suspension principle has to satisfy the following requirements:

- The strength of the roof bolts has to be greater than the relative weight of the loose roof layer that has to be carried.
- The anchorage forces of the roof bolts have to be greater than the weight of the loose roof layer.

The safety factor (SF_{sus}) of a bolting system in suspension mechanism is given by:

$$SF_{sus} = \frac{nP_f}{\rho g t_{lam}} \quad [7\text{-}11]$$

where, ρ = density of suspended strata (kg/m^3)

g = gravitational acceleration (m/sn^2)

P_f = resistance of bolting system calculated from SEPT (kN)

t_{lam} = thickness of loose layer or layers (m)

n = number of bolts/m^2

n can be calculated as follows:

$$n = \frac{k}{Ld} \quad [7\text{-}12]$$

where d = distance between the rows of roof bolts (m)

L = span (bord width) (m)

k = number of bolts in a row

7.4.2 Beam building mechanism

Classical beam theory was first used by Obert and Duvall (1967) in the design of roof bolt patterns. However, the derivations in this chapter are taken directly from a standard reference (Popov, 1978) to establish an improved design methodology for the beam building mechanism, which takes into account, where appropriate, the surcharge load (assumed to be parabolic) generated by the softened section above the bolted horizon. This phenomenon has been ignored in the design of roof support systems since 1970s by the introduction of beam building mechanism in South Africa.

The first consideration in the design of beam building mechanism is to determine the minimum required thickness of the beam which will be stable from the tensile failure point of view.

The maximum tensile stress must be smaller than the tensile strength of upper layer of built beam with an appropriate PoS (99 per cent). The maximum tensile stress in a built-beam with a parabolic surcharge load can be calculated as:

$$\sigma_{xx}\left(\pm\frac{L}{2}\right) = \frac{2}{5}\frac{\rho g L^2}{h^2}(h + h_1) \quad [7\text{-}13]$$

The tensile stress in the lower surface at mid-span of built-beam is:

$$\sigma_{xx}(0) = \frac{9}{40}\frac{\rho g L^2}{h^2}(h + h_1) \quad [7\text{-}14]$$

Beams are subjected to transverse loads which generate both bending moments $M(x)$ and shear forces $V(x)$ along the beam. The bending moments cause horizontal stresses, σ_{xx}, to arise through the depth of the beam, and the shear forces cause transverse shear-stress distributions $\tau_{xy} = \tau_{yx}$ through the beam cross section as shown in Figure 7-9.

An important consideration in beam theory is that the top and bottom surfaces of the beam are free of shear stress, and the shear stress distribution across the beam is parabolic. As a consequence of this, the maximum shear stress (at the neutral axis of the beam) is given by:

$$\tau_{\max}(x) = \frac{3V(x)}{2A} \qquad [7\text{-}15]$$

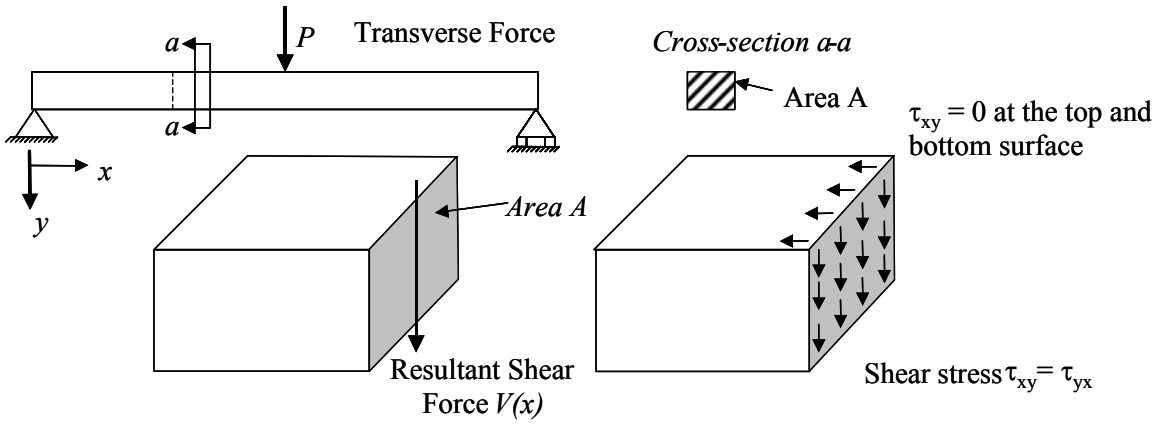

Figure 7-9 Beam with transverse shear force showing the transverse shear stress developed by it

The shear force distribution $V(x)$ is zero at the centre of a symmetrically loaded beam, and rises to a maximum at the end where it equals ½ of the total load. If the composite beam thickness is taken to be equal to the bolt length h, and the surcharge is parabolically distributed with a maximum height $h + h_1$ (Figure 7-8 and Figure 7-10), then

$$V_{\max} = \frac{1}{3}\rho g(h + h_1)L \qquad [7\text{-}16]$$

And from Equation [7-15]:

$$\tau_{\max} = \frac{1}{2}\frac{\rho g}{h}(h + h_1)L \qquad [7\text{-}17]$$

Where h = built beam thickness (m)

h_1 = additional surcharge thickness (m)

L = span (m)

ρ = density of strata (kg/m^3)

g = gravitational acceleration (m/s^2)

For the built composite beam to act as a single entity, the shear stress given by Equation [7-17] has to be overcome by the action of the bolts. Two types of resistance are provided: frictional due to bolt pre-tensioning, and intrinsic shear strength of the bolts.

Neglecting the inter-layer cohesion and layer deadweight, the frictional shear resistance of tensioned roof bolts can be calculated using the following well-known formula (Wagner, 1985):

$$T_R = nF_p\mu \qquad [7\text{-}18]$$

where n is number of bolts per square meter, F_p is the pre-tension of bolt (usually 50 kN), and μ is the coefficient of friction between the layers.

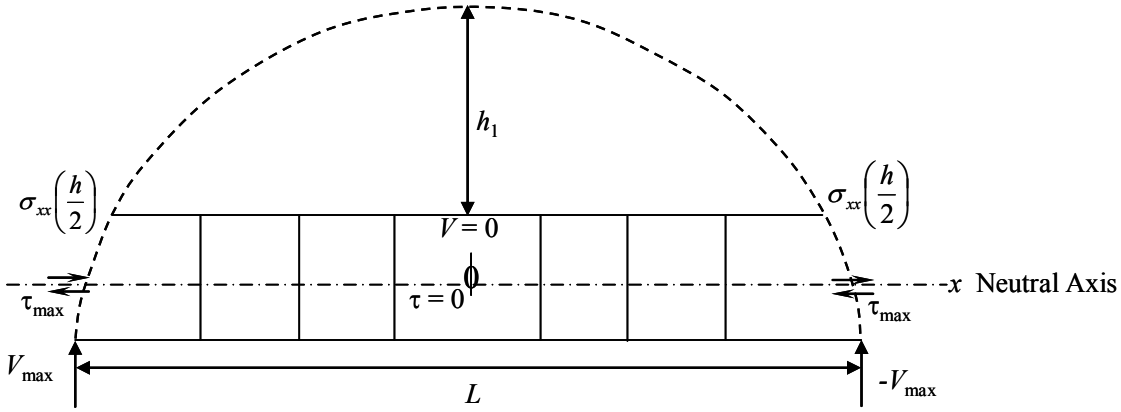

Figure 7-10 Computation and distribution of shear stress in a beam

In order to determine the coefficient of friction between the layers, a number of borehole samples from 5 collieries were obtained. All samples (61 mm in diameter and approximately 300 mm in length) were collected from the expoloration drilling and wraped in plastic bags to avoid weathering. To ensure for the failure to take place at the contacts between the different rock types, the top and bottom parts of the samples were cut and placed in a shear box. As shown in Table 7-5, the rock types and the contact conditions varied widely.

Despite the variation in rock and contact types, the standard deviation of the friction angle is relatively low: 9.2 per cent of the average. Note that the samples as tested may have been influenced by the drilling process. The influence of this has not been determined.

The shear strength of bolts also generates shear resistance, which must be considered in the design. This can be calculated using the following formula:

$$T_B = nS_R \qquad [7\text{-}19]$$

where S_R is shear strength of a bolt (in kN).

Table 7-5 Results of shear box tests on various contacts typically found in coal mines

Number	Contact details	Friction angle (deg.)	Coefficient of friction
1	coal/sandstone	23.6	0.44
2	shale/sandstone	24.3	0.45
3	coal/shale	24.8	0.46
4	shale/sandstone	21.7	0.40
5	shale/sandstone	24.7	0.46
6	shale/sandstone	29.8	0.57
7	coal/sandstone	25.8	0.48
8	coal/sandstone	25.8	0.48
9	sandstone/carbonaceous sandstone	24.3	0.45
10	coal/shale	22.9	0.42
11	sandstone/carbonaceous shale	25.1	0.47
12	coal/carbonaceous shale	23	0.42
13	sandstone/carbonaceous shale	20.2	0.37
14	coal/coal	27.8	0.53
15	coal/calcite	26.8	0.51
16	sandstone/carbonaceous shale	22.7	0.42
17	coal/sandstone	27.7	0.53
18	coal/sandstone	25.1	0.47
19	coal/laminated sandstone	25.2	0.47
Average		**24.8**	**0.46**
Standard deviation		**2.3**	**0.05**
Standard deviation as a percentage of average		**9.2**	**10.4**

There have been extensive studies in the past to determine the shear strength of a bolt. In South Africa, it has previously been accepted that 50 per cent of the *ultimate* tensile strength (UTS) of a bolt is approximately equal to the shear strength of a bolt (Wagner, 1985). However, Azuar (1977) concluded, from tests of resin-grouted bolts embedded in concrete, that the shear resistance of a joint when the bolt is installed perpendicular to the joint, is about of 90 per cent of the UTS. Roberts (1995) reported shear test results for smooth bars, rebars and cone bolts. He compared results of shearing at two interfaces (double shear) to a single interface shear and found that the former was not simply double the latter, as true symmetry did not exist in the case of double shear. Shear failure would occur at one interface first and subsequently resulted in failure of the other interface. From tests, he noted that a 16 mm diameter rebar had a static shear strength of approximately 90 per cent of the UTS. Canbulat et al. (2006), based on laboratory shear tests, also concluded that the shear strength of full-column roof bolts that are currently being used in South Africa is approximately 87 per cent of the ultimate tensile strength with very consistent results. Since this simple assumption will determine the required bolt length and density, it is suggested that the shear strength of a full column bolt is taken to be equal to

90 per cent of the UTS of a bolt (based on 600 MPa for standard roof bolts in South African collieries e.g. 190 kN for 20 mm bolts).

Equation [7-19] then becomes:

$$T_B = 0.9nS_B \qquad [7\text{-}20]$$

where S_B is the ultimate tensile strength of a bolt (in kN).

The shear resistance of a bolting system can therefore be determined as follows:

$$T_{TOTAL} = n(F_p\mu + 0.8S_B) \qquad [7\text{-}21]$$

And for stability this has to exceed the value given by Equation [7-17].

$$SF = \frac{T_{TOTAL}}{\tau_{\max}} \qquad [7\text{-}22]$$

Another important consideration in beam building mechanism occurs when the roof softening height is within the bolted horizon (Figure 7-11). This usually occurs when the bolts are installed late and the separation has already taken place and destroyed the cohesion between the layers or under excessive stress conditions.

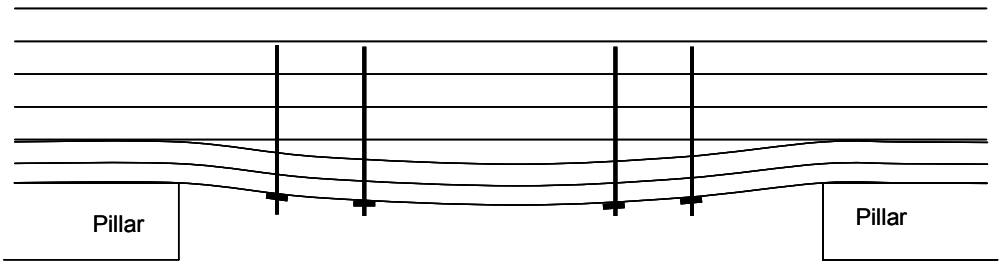

Figure 7-11 Bed separation within the bolted horizon

In this case, safety factor (SF_{slide}) of resistance to sliding of the bolting system should be calculated using the bond strength (B_s) between the resin, rock and the bolt using the following formula:

$$SF_{slide} = \frac{kB_S l_{cap}}{Lt_{loose}d\rho g} \qquad [7\text{-}23]$$

Where B_S = Bond strength or grip factor (kN/mm)
d = distance between the rows of roof bolts (m)
L = span (bord width) (m)
t_{loose} = thickness of separated layer (m)
k = number of bolts in a row
l_{cap} = capsulation length (bolt length – t_{loose}) (m)
ρ = density of strata (kg/m^3)

g = gravitational acceleration (m/s^2)

Bond strength is measured through short encapsulation pull tests (SEPT). In order to measure the bond strength, it is necessary to shear the bond on the bolt-resin or resin-rock interface. With the modern high-strength, high-stiffness, polyester resins, it has been found that a bond length of 250 mm is appropriate for determining the bond strength.

Bond strength (B_S) is defined as:

$$B_S = \frac{Maximum\,Load\,Achieved\,(kN)}{Encapsulation\,Length\,(mm)} \qquad [7\text{-}24]$$

Similar to suspension mechanism, to avoid the failure of roof bolts in tension, the safety factor (SF_{bolt}) of roof bolts should also be determined. The following formula can be used to calculate the safety factor of roof bolts:

$$SF_{slide} = \frac{kP_{bolt}}{Lt_{loose}d\rho g} \qquad [7\text{-}25]$$

Where P_{bolt} = bolt yield strength (kN)
d = distance between the rows of roof bolts (m)
L = span (bord width) (m)
t_{loose} = thickness of separated layer (m)
k = number of bolts in a row
ρ = density of strata (kg/m^3)
g = gravitational acceleration (m/s^2)

7.5 Determination of stability of the immediate layer between the roof bolts

In the case of thin roof beds the spacing between bolts is critical. Wagner (1985) suggested that the distance between the bolts should not exceed a value of 10 times the thickness of the layer. However, to prevent the failure of the immediate roof between the bolts, the tensile stress between the bolts for the immediate layer may be calculated by assuming that the bolts create a fixed beam between them. If the tensile stress between the bolts exceeds the tensile strength of the material then the distance between the bolts should be reduced or an areal coverage system should be used. The safety factor of roof between the bolts may be calculated again from the clamped beam equation (van der Merwe and Madden, 2002):

$$SF = \frac{2t_{imm}^2\,\sigma_x}{\rho g t_{imm} L_b^2} \qquad [7\text{-}26]$$

where, σ_x = tensile strength of immediate roof (MPa)

ρ = density of immediate layer (kg/m^3)

g = gravitational acceleration (m/s^2)

L_b = distance between the bolts (m)

t_{imm} = thickness of immediate layer (m)

Note that in the case of low modulus layers overlaying the immediate layer, surcharge loading should be taken into account by suitably increasing t in the numerator of Equation [7-26].

In the case of failure of very thin layers (<100 mm) between the roof bolts, it is certainly impossible to prevent the failure using only roof bolts, in this case, if the layer cannot be mined out due to contamination concerns, areal coverage in the form of wire-mesh, W-straps and/or shotcrete is recommended.

7.6 Probability density functions of design parameters and random selection

As indicated in Section 7.2 that the fundamental to Monte Carlo method is the process of explicitly representing the uncertainties by specifying inputs as probability distributions. Probability density functions are the tools used to estimate the likelihood that random variable values will occur within certain ranges. There are two types of random variables, namely discrete and continuous. A discrete (finite) random variable can take only a countable number of distinct values. A continuous (infinite) random variable can however takes an unknown number of possible samples and the samples are not countable, but are taken from a continuous interval. Because few, if any, geotechnical properties will behave as a discrete probability space, discrete distributions are not presented herein.

The probability density function is a function that assigns a probability to every interval of the outcome set for continuous random variables. The probability density function is denoted $f_x(x)$, where x is the random variable itself and x is the value that the continuous random variable can take on. Probability functions have the following properties (Jones et al., 2002):

1. The function is always nonnegative, $f_x(x) \geq 0$
2. The area under the function is equal to one, $\int_{-\infty}^{\infty} f_x(x)dx = 1$

3. The probability that a random value, X, from the distribution is between a and b is

$$P[a \le x \le b] = \int_a^b f_x(x)dx$$

Cumulative probability distribution (CDF) functions have the value at x_0 corresponding to the probability that a random value, X, from the distribution will be less than or equal to x_0.

For a continuous distribution, this can be expressed mathematically as $\Pr(X \le x_0 = \int_{-\infty}^{x_0} f(x)\,dx$

Over 25 special continuous probability density distributions exist. The following 10 most commonly used distributions are however utilised in this thesis:

1. Beta
2. Erlang
3. Exponential
4. Gamma
5. Logistic
6. Lognormal
7. Normal
8. Pert
9. Weibull

Rather than focus on the derivations, useful properties of these distributions are presented in Table 7-6.

In order to determine the best fit probability density distributions for each of the input parameters used in the design, the underground measurement data collected throughout this study has been analysed using the Anderson-Darling goodness of fit test.

Table 7-6 Summary of probability distributions (after EasyFit user manual, 2006)

Distribution	Parameters	Density distribution function	Cumulative distribution function	Definitions
Beta	α_1 continuous shape α_2 continuous shape	$f(x)=\frac{x^{\alpha_1-1}(1-x)^{\alpha_2-1}}{B(\alpha_1,\alpha_2)}$	$F(x)=\frac{B_x(\alpha_1,\alpha_2)}{B_x(\alpha_1,\alpha_2)}\equiv I_x(\alpha_1,\alpha_2)$	B = Beta function B_x = Incomplete beta function
Erlang	m integral shape β continuous scale	$f(x)=\frac{1}{\beta(m-1)!}\left(\frac{x}{\beta}\right)^{m-1}e^{-x/\beta}$	$F(x)=\frac{\Gamma_{x/\beta}(m)}{\Gamma(m)}=1-e^{-x/\beta}\sum\frac{(x/\beta)^i}{i!}$	Γ = Gamma function Γ_x = Incomplete gamma function
Exponential	β continuous scale	$f(x)=\frac{e^{-x/\beta}}{\beta}$	$F(x)=1-e^{-x/\beta}$	
Gamma	α continuous shape β continuous scale	$f(x)=\frac{1}{B\Gamma(x)}\left(\frac{x}{\beta}\right)^{\alpha-1}e^{-x/\beta}$	$F(x)=\frac{\Gamma_{x/\beta}(\alpha)}{\Gamma(\alpha)}$	Γ = Gamma function Γ_x = Incomplete gamma function
Logistic	α continuous location β continuous scale	$f(x)=\frac{\sec h^2\left[\frac{1}{2}\left(\frac{x-\alpha}{\beta}\right)\right]}{4\beta}$	$F(x)=\frac{1+\tan h\left[\frac{1}{2}\left(\frac{x-\alpha}{\beta}\right)\right]}{2}$	$sec\ h$ = hyperbolic Secant Function $tan\ h$ = hyperbolic Tangent Function
Lognormal	μ continuous σ continuous	$f(x)=\frac{1}{x\sqrt{2\pi}\sigma'}e^{-\frac{1}{2}\left[\frac{\ln x-\mu'}{\sigma'}\right]^2}$	$F(x)=\Phi\left(\frac{\ln x-\mu'}{\sigma'}\right)$	$\mu'\equiv\ln\left[\frac{\mu^2}{\sqrt{\sigma^2+\mu^2}}\right]$ $\sigma'\equiv\sqrt{\ln\left[1+\left(\frac{\sigma}{\mu}\right)^2\right]}$ $\Phi(z)$ = Laplace-Gauss

Distribution	Parameters	Density distribution function	Cumulative distribution function	Definitions
				integral
Normal	α continuous location β continuous scale	$f(x)=\frac{1}{\sqrt{2\pi}\sigma'}e^{-\frac{1}{2}\left[\frac{x-\mu}{\sigma}\right]^2}$	$F(x)=\Phi\left(\frac{\ln x-\mu}{\sigma}\right)=\frac{1}{2}\left[erf\left(\frac{x-\mu}{\sqrt{2}\sigma}\right)+1\right]$	Φ = Laplace-Gauss integral *erf* = error function
Pert	$\mu\equiv\frac{\min+4\,m.likely+\max}{6}$ $\alpha_1\equiv 6\left[\frac{\mu-\min}{\max-\min}\right]$ $\alpha_2\equiv 6\left[\frac{\max-\mu}{\max-\min}\right]$	$f(x)=\frac{(x-\min)^{\alpha_1-1}(\max-x)^{\alpha_2-1}}{B(\alpha_1,\alpha_2)(\max-\min)^{\alpha_1+\alpha_2-1}}$	$F(x)=\frac{B_z(\alpha_1,\alpha_2)}{B(\alpha_1,\alpha_2)}\equiv \mathrm{I}_z(\alpha_1,\alpha_2)$	min = continuous boundary parameter (min < max) m.likely = continuous parameter (min<m.likely<max) max = continuous parameter $z\equiv\frac{x-\min}{\max-\min}$ B = Beta function B_z = Incomplete beta function
Weibull	α continuous shape β continuous scale	$f(x)=\frac{\alpha x^{\alpha-1}}{\beta^{\alpha}}e^{-(x/\beta)^{\alpha}}$	$F(x)=1-e^{-(x/\beta)^{\alpha}}$	

7.6.1 Goodness of fit tests

There are several goodness of fit tests available, among them Kolmogorov-Smirnov (KS-test), Chi-square (CS-test) and Anderson-Darling (AD-test) goodness of fit tests.

Kolmogorov-Smirnov (Chakravart et al., 1967) test determines if two datasets differ significantly. An advantage of KS-test is that the distribution of the KS-test statistic itself does not depend on the underlying cumulative distribution function being tested. Another advantage is that unlike chi-square test, it is an exact test and does not require binned data an adequate sample size for the approximations to be valid. Despite these advantages, the KS-test has several important limitations:

1. It tends to be more sensitive near the centre of the distribution than at the tails.
2. The distribution must be fully specified. That is, if location, scale, and shape parameters are estimated from the data, the critical region of the KS-test is no longer valid. It typically must be determined by simulation.

The chi-square goodness of fit test (Snedecor and Cochran, 1989) is used to test if a sample of data came from a population with a specific distribution.

An important feature of the CS-test is that it can be applied to any distribution for which the CDF can be calculated. The chi-square goodness-of-fit test can only be applied to binned data (i.e., data put into classes) and the value of the chi-square test statistic is dependent on how the data is binned. Another disadvantage of the chi-square test is that it requires a sufficient sample size in order for the chi-square approximation to be valid. The test requires that the data first be grouped. The actual number of observations in each group is compared to the expected number of observations and the test statistic is calculated as a function of this difference.

Anderson-Darling test is a general test to compare the fit of an observed cumulative distribution function to an expected cumulative distribution function and can be applied to binned and unbinned data. AD-test is a modification of the KS-test and gives more sensitive to deviations in the tails of the distribution. The AD-test makes use of the specific distribution in calculating critical values. This has the advantage of allowing a more sensitive test and the disadvantage of that critical values must be calculated for each distribution.

Since the the Anderson-Darling test implemented in EasyFit© (a computer program which determines the best fits based on goodness of fit tests) uses the same critical values for all the distributions and these values are calculated using the approximation formula, depending on the sample size, Anderson-Darling goodness of fit test and EasyFit© are utilised in this thesis to determine the best probability distributions representing the input parameters

The Anderson-Darling statistic (A^2) is defined as: (EasyFit© user manual, 2006)

$$A^2 = -n - \frac{1}{n}\sum_{i=1}^{n}(2i-1)\left[\ln F(X_i) + \ln(1 - F(X_{n-1+i}))\right] \qquad [7\text{-}27]$$

The hypothesis regarding the distributional form is rejected at the chosen significance level (α) if the test statistic, A^2, is greater than the critical value.

7.6.2 Probability distributions of design parameters

Based on the load/strength models presented in Section 7.3 and 7.4, the following parameters' probability distributions will be determined to use in the probabilistic design of roof bolting systems:

- Bord width
- Distance between the bolts (in determining the roof bolt density)
- Pre-tension of roof bolts
- Height of roof softening
- Unit weight
- Bond strength
- Coefficient friction
- Bolt strength
- Tensile strength of rock
- Thickness of competent layer
- Thickness of suspended layer

Note that the distribution of roof bolt strength is calculated from the variation in the diameter of 18 mm roof bolts using a constant ultimate steel strength of 600 MPa.

A summary of the goodness of fit test results using the AD-test is summarised in Table 7-7.

Table 7-7 Summary results of Anderson-Darling goodness of fit tests

Parameter	Number of data points	Best fit probability distribution	Scale Parameter	Shape Parameter	Location parameter
Bord width (m)	258	Logistic	0.32	N/A	6.23
Distance between the bolts (m)	835	Pert	1.90 (mode)	0.58 (min)	3.31 (max)
Pre-tension of roof bolts (kN)	122	Pert	29.80 (mode)	18.92 (min)	82.50 (max)
Height of roof softening (m)	93	Logistic	0.17	N/A	0.65
Unit weight (MN/m^3)	168	Erlang	16.24	148.00	N/A
Bond strength (kN/mm)	46	Lognormal	0.29	N/A	-0.87
Coefficient friction (^{o})	19	Lognormal	0.10	N/A	-0.78
Bolt strength (kN)	192	Logistic	0.36	N/A	120.40
Tensile strength of sandstone (MPa)	30	Pert	3.15 (mode)	0.46 (min)	5.19 (max)
Tensile strength of weak rock (MPa)	66	Pert	0.79 (mode)	0.32(min)	3.44 (max)
Thickness of competent layer (m)	43	Weibull	2.60	2.84	N/A
Thickness of suspended layer (m)	43	Normal	0.20	N/A	0.89

Note that as can be seen, the results presented in Table 7-7 are based on a limited number of data points. Therefore, certain best fit probability distributions obtained from Anderson-Darling goodness of fit tests are only marginally better than the others, such as Weibull distribution is only slightly better than the normal distribution for the thickness of the competent layer. This indicates that a more comprehensive database is required to establish the conclusive distributions.

7.7 Support design methodology

Using all above and the information presented in other Chapters of this thesis, the following step-by-step process is suggested in the design of roof support system:

1. Conduct a detailed geotechnical analysis to determine the height of roof softening. This can be achieved for existing operations from underground measurements and/or height of FOG, and for greenfield studies from the geotechnical rating systems (such as IST, CMRR and RQD). The details of these investigations can be found in Chapters 3, 4, 5, 6 and 7.

2. Determine the applicability of the suspension mechanism using Equation [7-10]. Note that a minimum PoS of 99 per cent is recommended to use the suspension mechanism with confidence.

3. Further detailed geotechnical analyses are required to determine the distributions of suspension and beam building mechanisms' input parameters. These input parameters and their probability distributions are summarised in Chapter 7.

4. Conduct short encapsulated pull tests to calculate the support resistance. Use the standard ISRM SEPT methodology.

5. For the appropriate support mechanism calculate the probability of stabilities of different length of roof bolts. Note that if required a sensitivity analysis into the distance between the rows of support elements, bord width, bond strength and pre-tension on roof bolts can be conducted at this stage. The details of this analysis can be found in Chapter 7.

6. Check the probability of stabilities achieved against the design criteria given in Table 7-4. If the design criteria is not achieved go back to Step 4.

7. If the design criteria is achieved in Step 7, check the stability between the roof bolts using Equation [7-26].

8. Determine the financial viability of the system. If the system is financially viable, implement it; otherwise conduct a detailed analysis into different bolting systems in Step 5.

9. Once the bolting system is implemented (i) monitor the support system and (ii) implement the appropriate quality control procedures using the methodology presented in Chapter 6.0.

10. As an on going procedure, use appropriate (developed for the specific conditions) section performance and risk rating system and continue monitoring the support system and the roof behaviour.

A design flow-chart summarising the above methodology is presented in Figure 7-12.

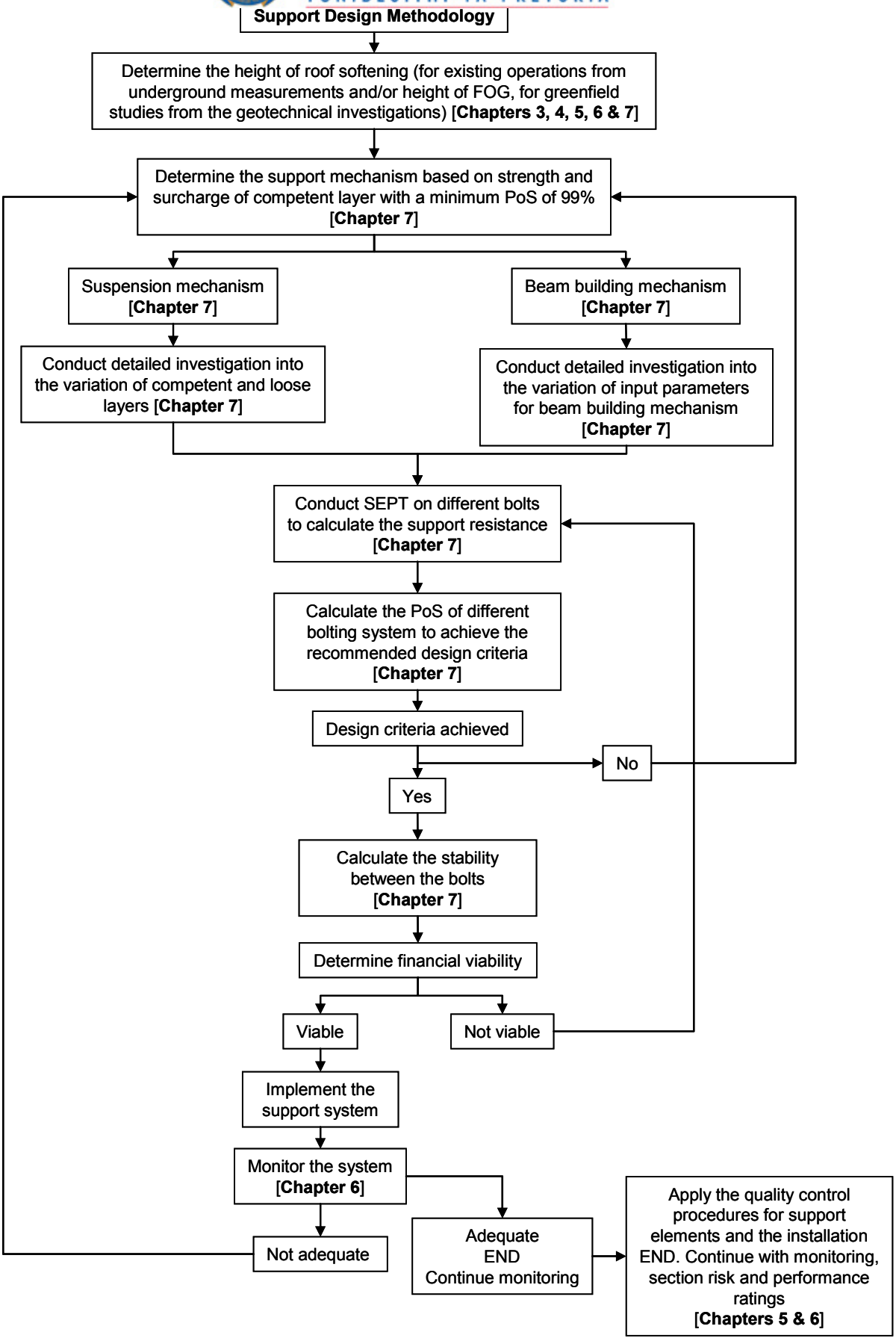

Figure 7-12 Recommended support design methodology

7.8 Application of the probabilistic design approach to a case study

In the previous sections of this Chapter, a probabilistic design methodology is presented. In this section a verification of this design methodology will be demonstrated by applying it to a well-defined study with the aim of establishing the best support systems for a colliery in the Witbank Coalfield.

A detailed monitoring program was conducted in a bord and pillar section of Colliery 'A'. Using three sonic probe monitoring sites (two in roadways and one in an intersection) the roof behaviour was monitored and the height of roof softening data was obtained. Additional data was also obtained using a feeler-gauge (a telescopic pipe which contains a washer at the end and is inserted into a bolt hole to feel the bed separations). The mine experienced numerous roof falls for a period of time and an investigation into the thickness of roof falls was therefore conducted. This data was also combined with the sonic probe and fleer-gauge data to extend the height of roof softening database. Figure 7-13 summarises the data obtained from these three different techniques. It is evident from this Figure that the height of softening varies from 0.15 m to 1.65 m with an average of 0.65 m.

A detailed bord width measurement programme was also conducted and bord width offsets were measured in two different production sections. A frequency versus bord width graph is given in Figure 7-14. In these two sections, the bord widths were designed to be 6.5 m, but, in reality varied from 5.4 m to 7.6 m.

The immediate roof strata consisted of 0.1 to 1.0 m of coal, followed by a shale band approximately 0.3 m thick above which there is a further 3.0 m of coal. This data was obtained from 43 borehole logs that were available in the vicinity of the area where the bord width measurements and the height of roof softening data were collected. Figure 7-15 illustrates the distributions of thicknesses of the immediate and the upper roof coal layers. In this Figure, the immediate roof thicknesses included the skin coal and the shale band whilst the upper roof included the coal thickness overlain the immediate roof.

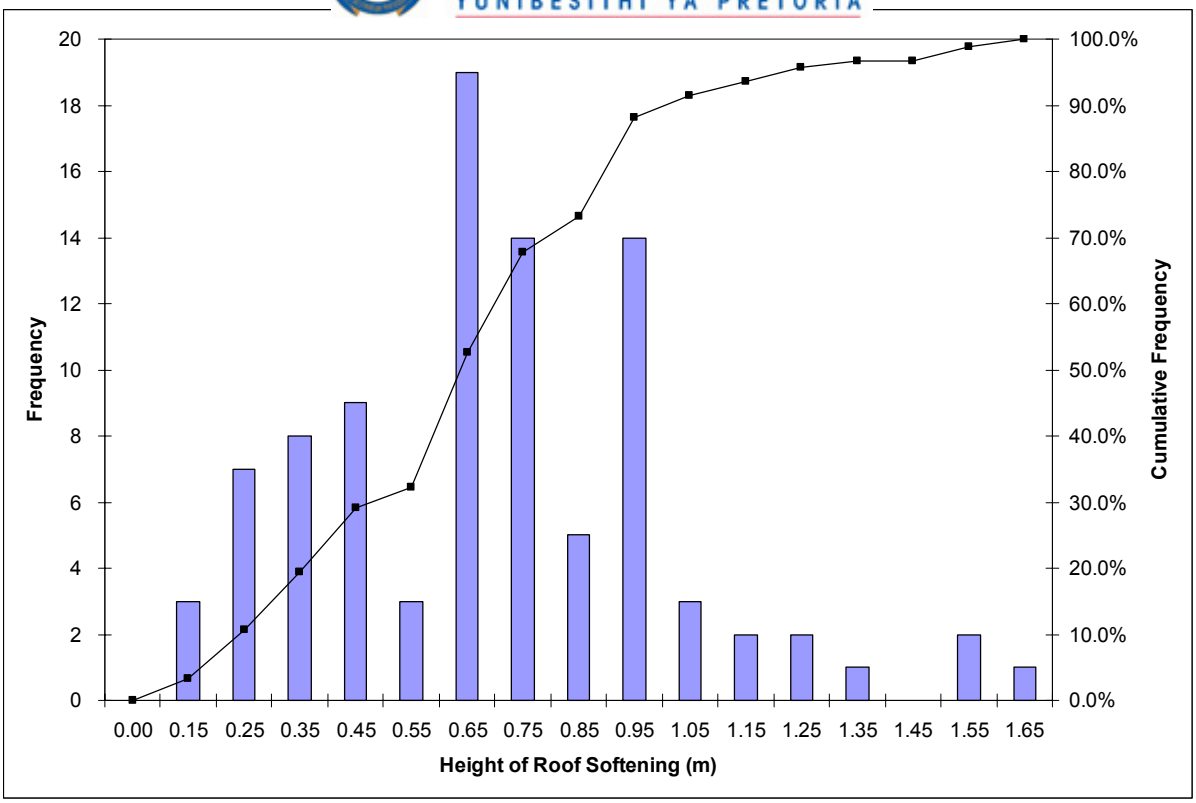

Figure 7-13 Colliery "A" height of softening data obtained from the sonic probe extensometer results, feeler-gauge results and FOG data

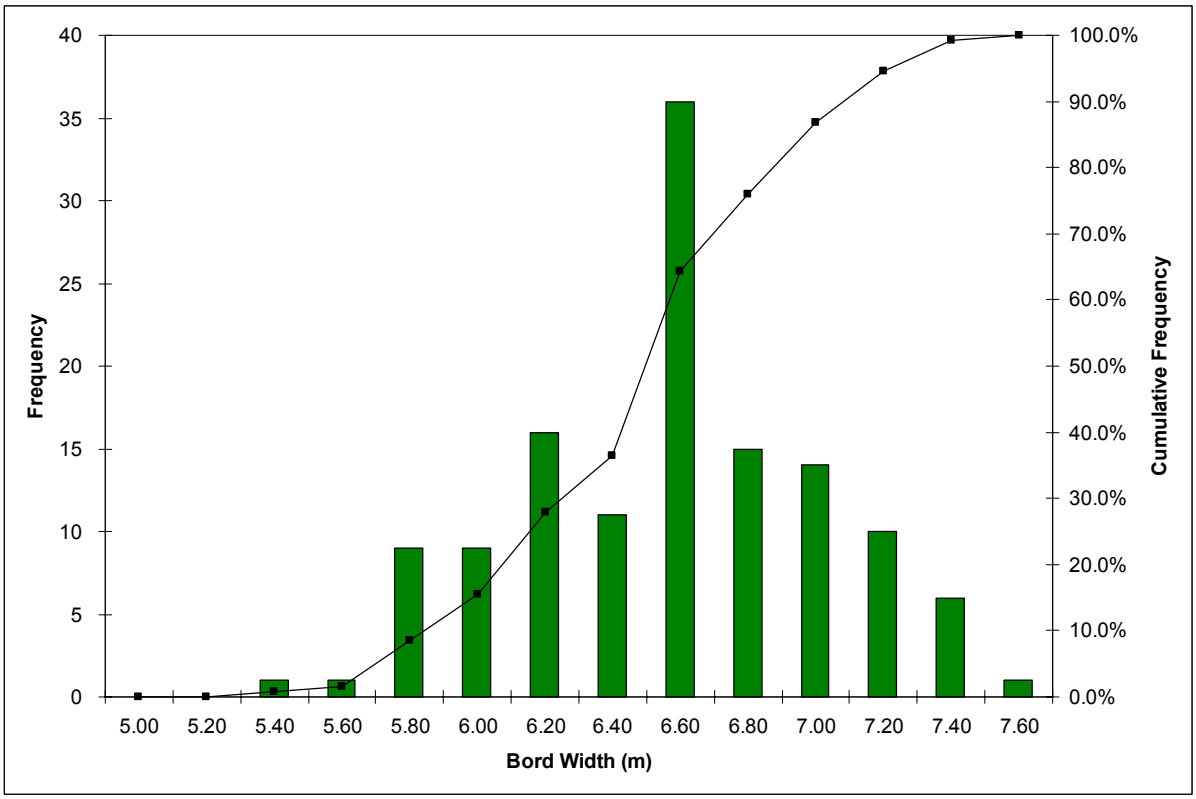

Figure 7-14 Bord width distributions in the experiment site

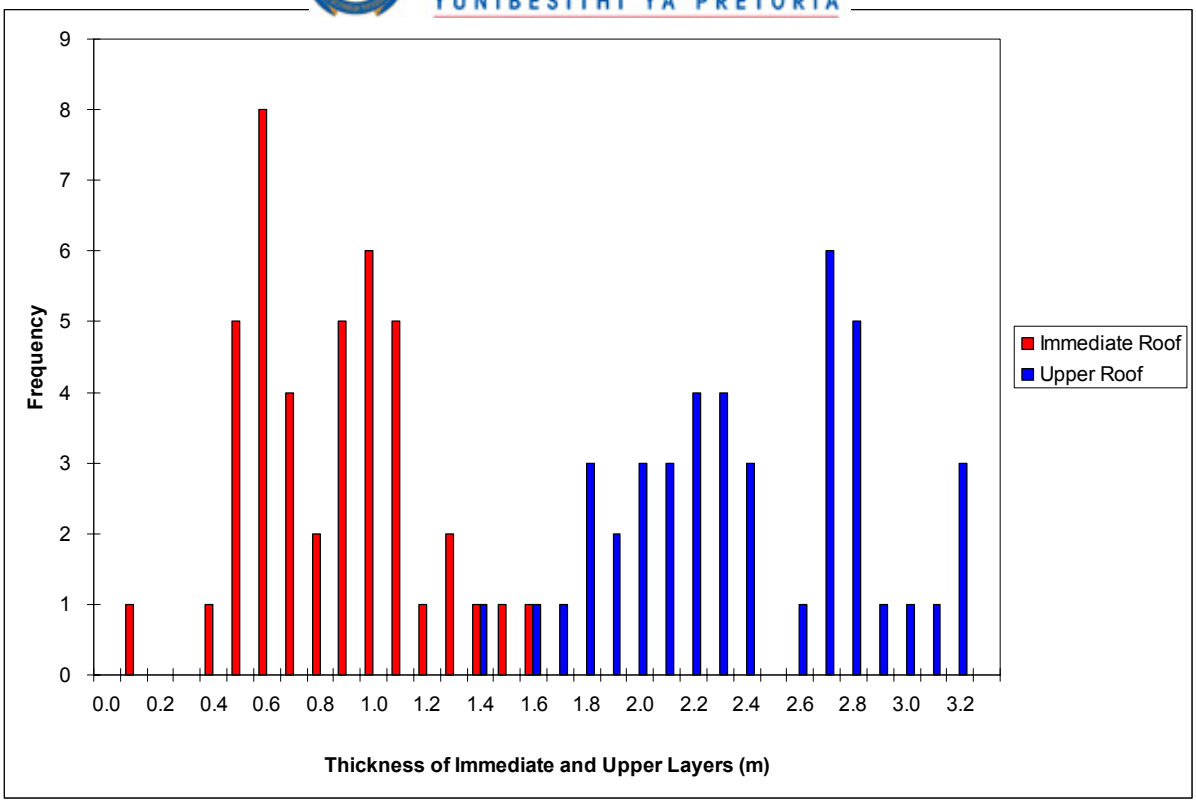

Figure 7-15 Thickness of immediate and upper roof obtained from borehole logs

A series of underground short encapsulation pull tests were carried out in near identical conditions in those two sections. Tests were performed using the 30 second spin and hold resin and 1.2 m long, 16 mm roof bolts, as currently being used by the mine. Note that due to the time laps between the tests and the need for the roofbolter in production schedule, tests were conducted in different areas of the sections.

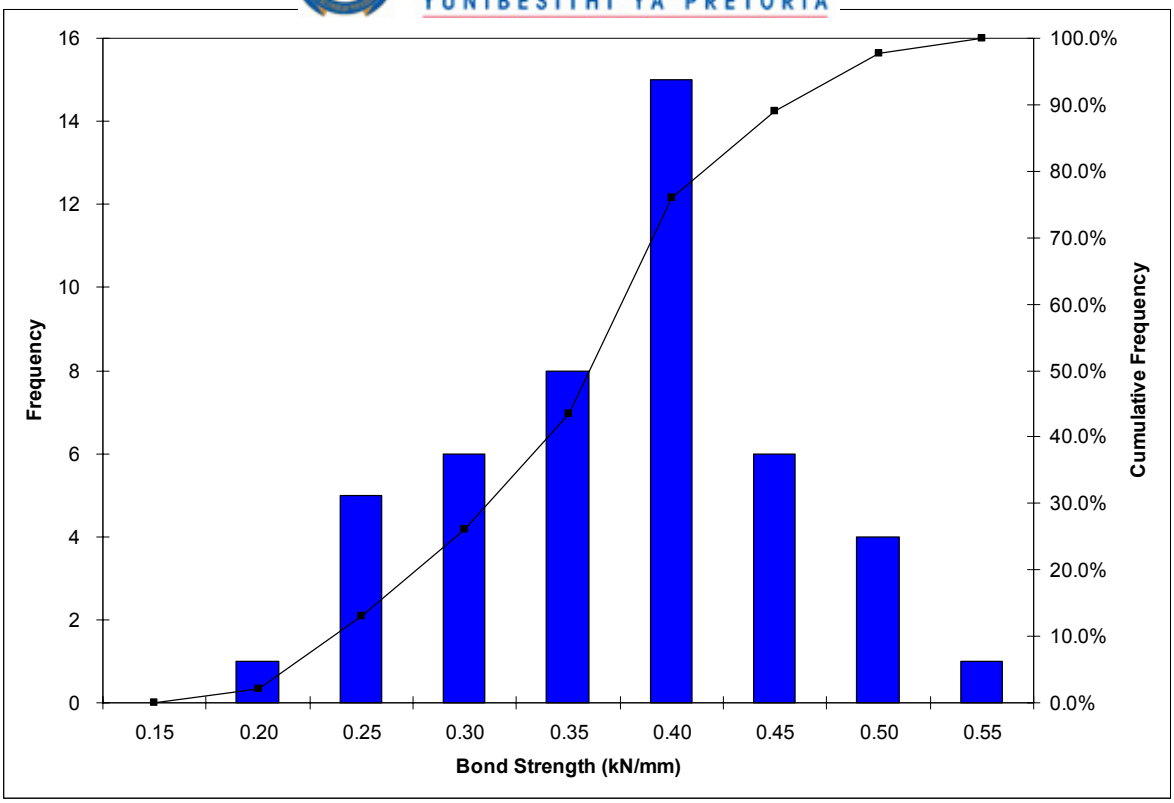

Figure 7-16 Bond strength results obtained from SEPT in the experiment site

In order to determine the tension on the roof bolts, over 145 roof bolts were tested using a torque-wrench. Figure 7-17 shows the distribution obtained from these measurements. As can be seen the tension on the roof bolts varied from 0 to 32.5 kN.

The distances between the rows of roof bolts were also measured in the monitoring site, Figure 7-18. Similar to bord widths, although the planned distance was 2.0 m, in reality it varied from 1.4 m to 3.2 m.

In order to determine the strength of roof bolts based on a constant 600 MPa ultimate steel strength, bolt diameter measurements were also taken over 80 bolts at the mine and the ultimate strength of roof bolts were determined, Figure 7-19.

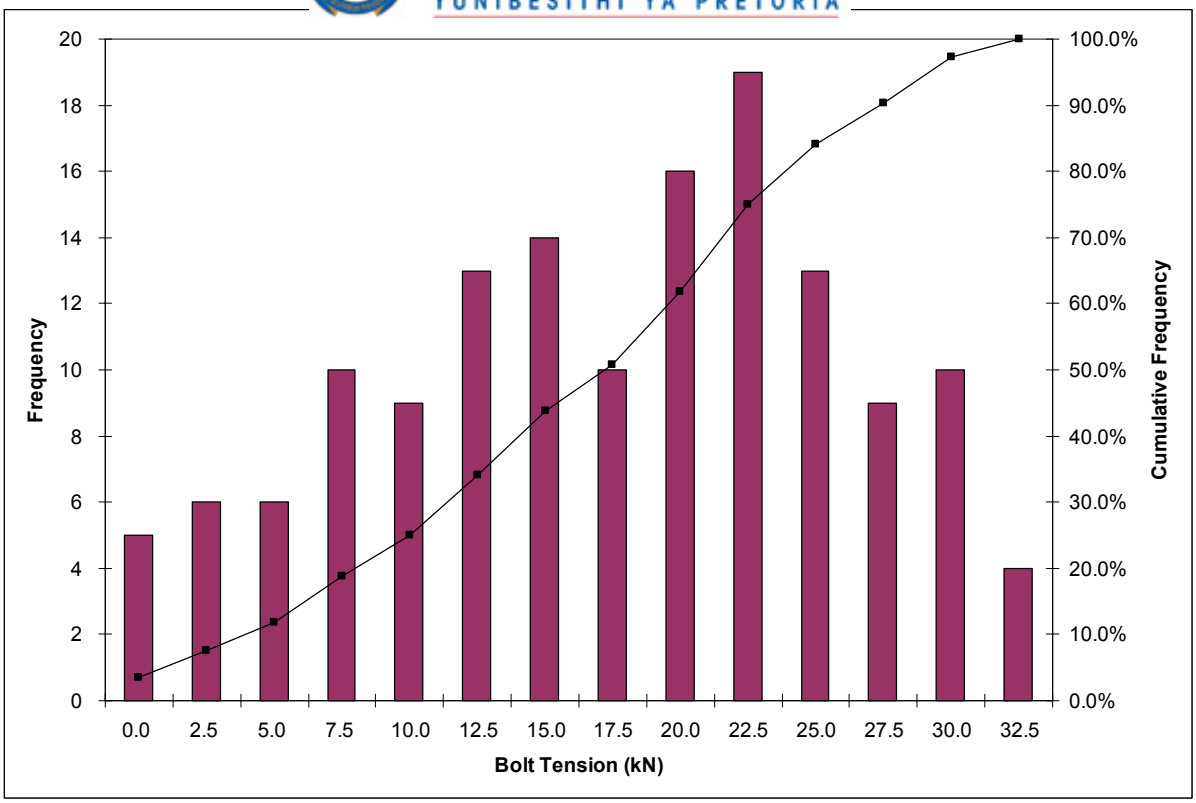

Figure 7-17 Distribution of roof bolting tensioning results

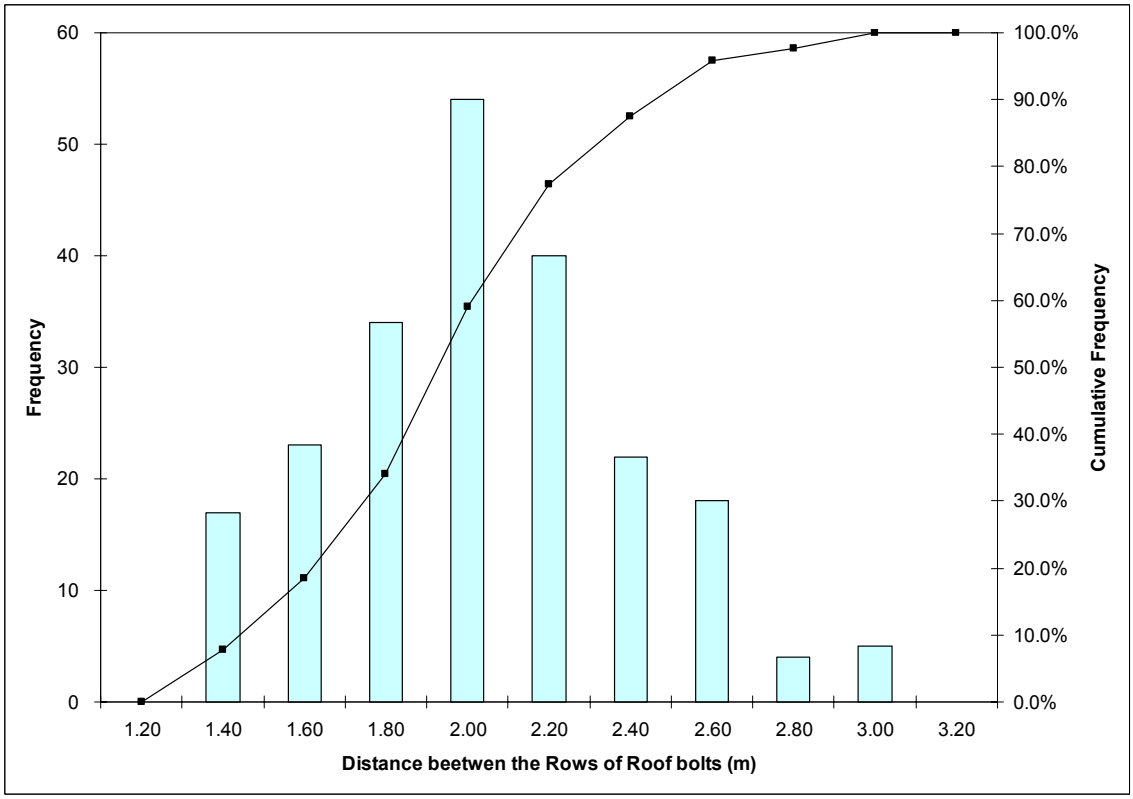

Figure 7-18 Distance between the roof bolts measured in the experiment site

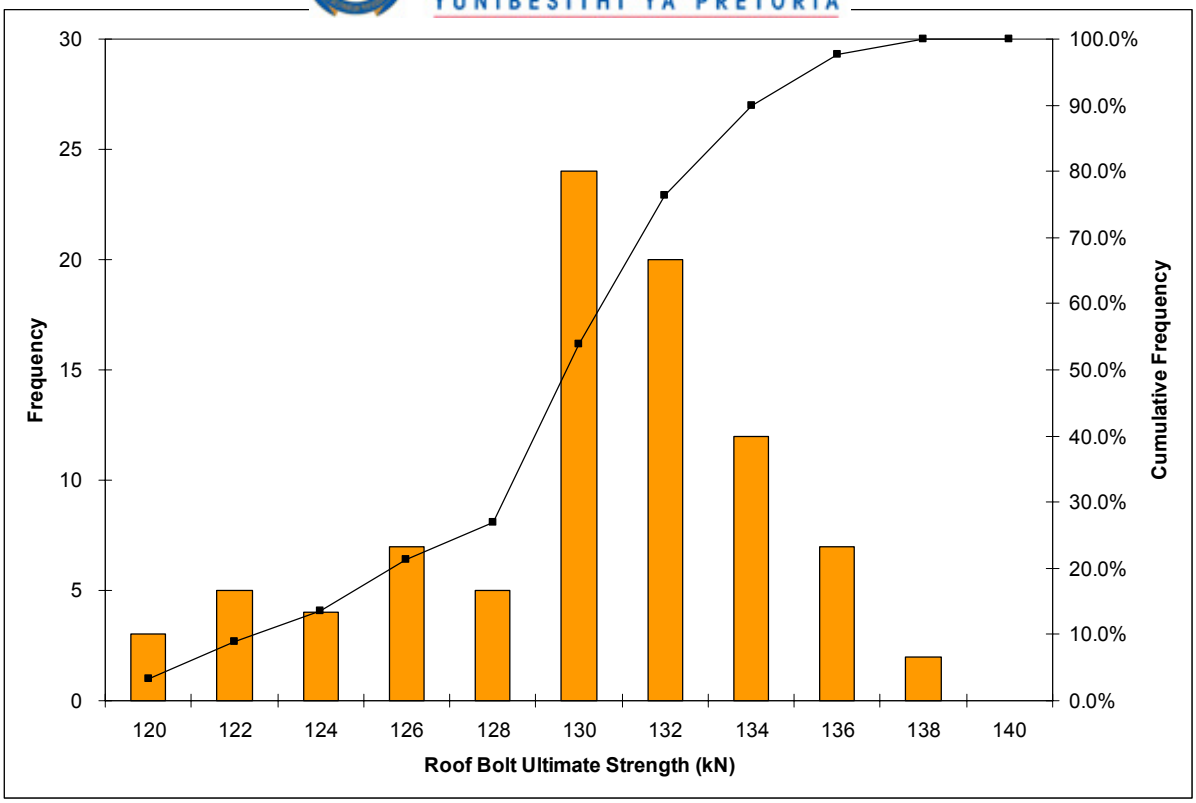

Figure 7-19 Roof bolt ultimate strength

An extensive laboratory testing programme was also initiated to determine the tensile strength of the immediate and upper coal layers with the aim of determining the applicability of suspension and beam building mechanisms as well as the stability of the immediate roof between the roof bolts. Additional information such as the unit weights of coal and shale were also determined from these laboratory tests. The distribution of tensile strength of coal as obtained from the Brazilian Tensile Strength tests is shown in Figure 7-20. Figure 7-21 shows the distribution of unit weights of the immediate and the upper coal layers determined from these laboratory tests.

Due to the lack of information at the mine regarding the coefficient of friction between the layers in the roof, the data presented in Table 7-5 was used in this study. Figure 7-22 illustrates the distribution of the data given in Table 7-5.

A summary of the information presented above is given in Table 7-8 together with the additional information obtained from the mine.

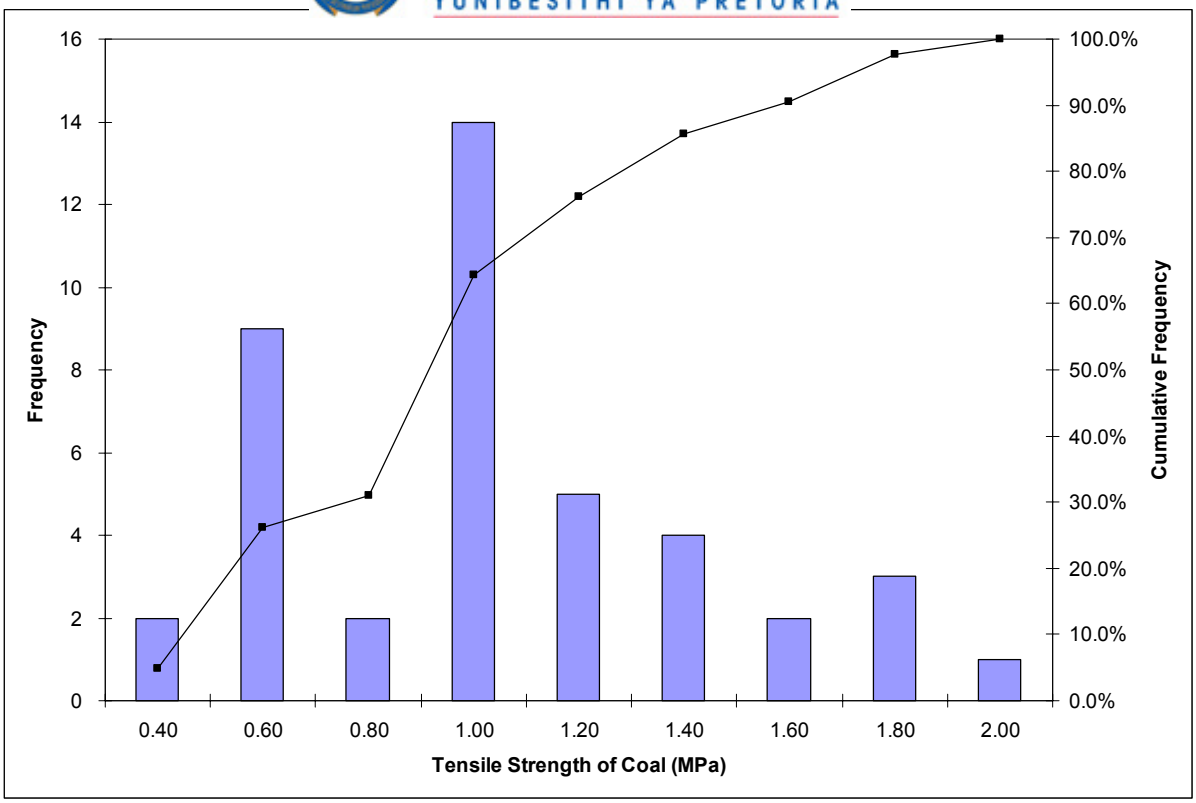

Figure 7-20 Distribution of tensile strength of coal used in the analysis

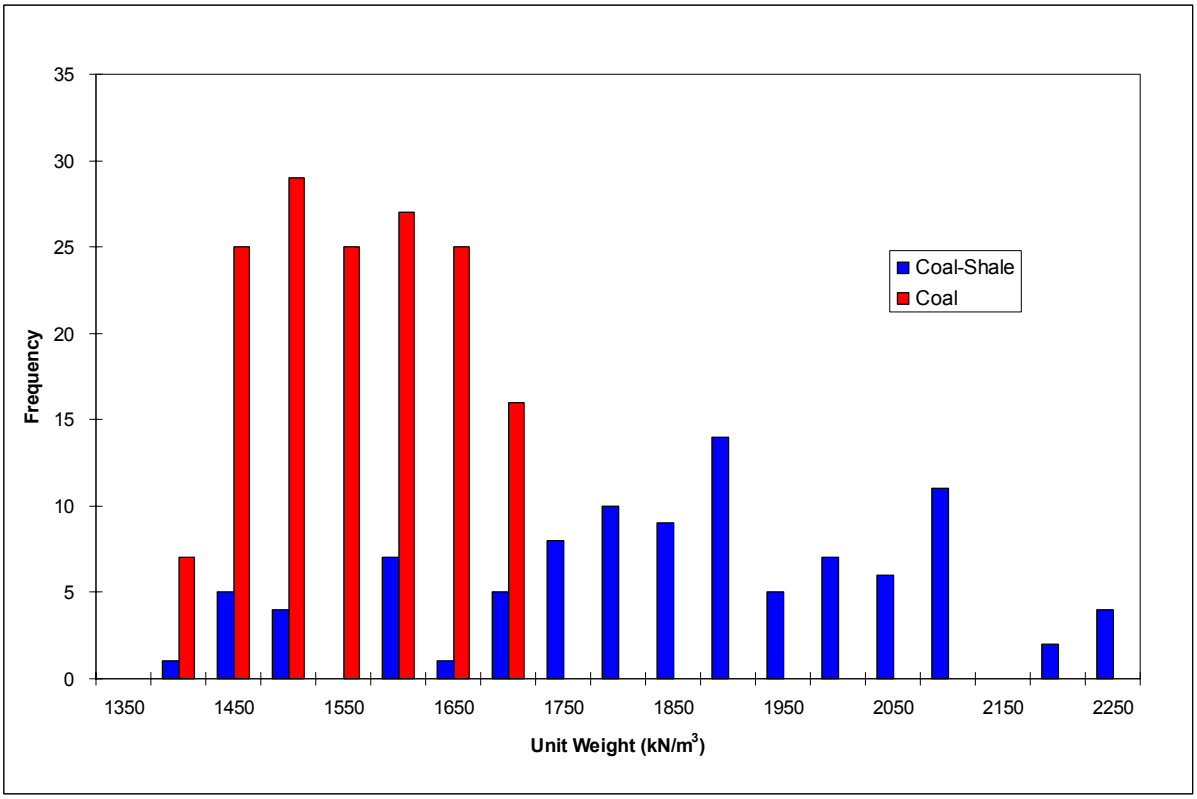

Figure 7-21 Unit weights of the immediate and upper coal layers

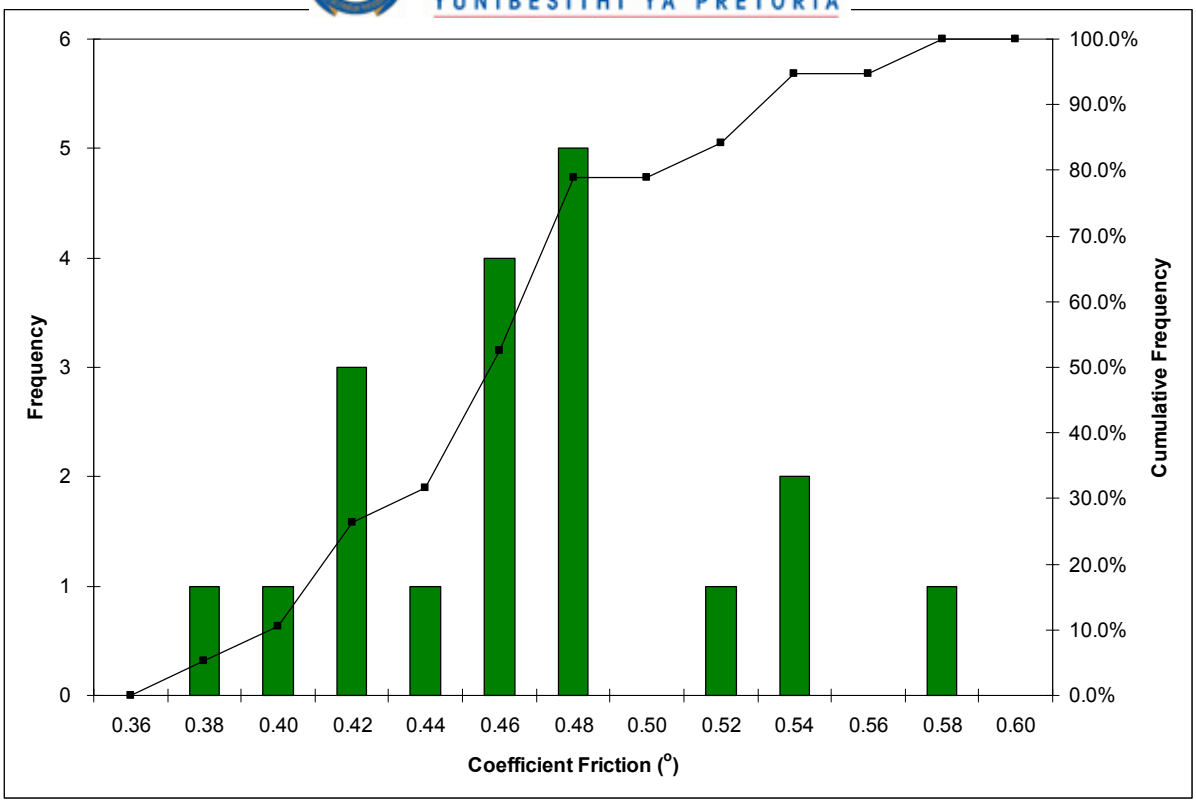

Figure 7-22 Distribution of coefficient of friction between the layers

Table 7-8 Summary of information used in the analysis

	Number of samples	Minimum	Maximum	Average	Mode
Height of roof softening (m)	93	0.2	1.6	0.7	0.6
Bord widths (m)	129	5.3	7.5	6.5	6.5
Thickness of immediate layer (m)	43	0.1	1.6	0.8	1
Thickness of upper coal layer (m)	43	1.5	3.3	2.5	2.1
Bond strength (kN/mm)	46	0.2	0.6	0.4	0.4
Bolt tensioning (kN)	145	0	32	16.4	20
Distance between the rows of roof bolts (m)	217	1.3	3	2	2
Roof bolt ultimate strength (m)	209	119.3	137.8	129.3	126
Unit weight of immediate layer (MN/m^3)	99	1382.8	2214.4	1835.3	1900
Unit weight of upper coal layer (MN/m^3)	154	1380.9	1669.7	1530.1	1531.2
Coal tensile strength (MPa)	40	0.4	1.8	1	1.2
Coefficient of friction between the layers	19	0.4	0.6	0.5	0.4
Coalfield	Witbank				
Seam	No 2				
Mining height	3.0 m				
Mining method	Continuous miner bord and pillar, 9 road section				
Depth	47 m				
Pillar widths	9.0 m				
Number of bolts in a row	3				
Cut out distance	8.0 m				

Regarding the input parameters presented above the following comments can be made:

- The input parameters can be divided into two distinct groups, namely uncontrollable parameters (representing the ground conditions, i.e. height of roof softening, thicknesses of the immediate and the upper roof layers, unit weight of rock, rock tensile strength and coefficient of friction between the layers) and controllable parameters (representing the mining practice, i.e. bord width, the distance between the roof bolts, bolt tensioning, strength of roof bolts).
- Uncontrollable parameters are the true reflection of ground conditions present and cannot be changed.
- Controllable parameters are however the true reflection of the responses to those conditions and can be changed/improved to increase the probability of stability of the roof bolting systems.

7.8.1.1 Results

In order to determine the support mechanism using the above input parameters, the applicability of the suspension mechanism, as applied by the mine, was investigated using the input parameters presented above. A total of 20,000 Monte Carlo simulations were run using Equation [7-10] and the results showed that although the average safety factor of upper coal layer is 1.79, the PoS of suspension mechanism is only 92.6 per cent with a Reliability Index of 0.53, which is not acceptable according to criteria set in Section 7.3.1 (i.e., the minimum required PoS should be 99 per cent to use the suspension mechanism with confidence). Figure 7-23 presents the distribution of safety factors for the stability of the upper coal layer using the probability distributions presented in Table 7-7.

Nevertheless, in order to demonstrate the probability of failure using the suspension mechanism with the input parameters presented above, a further study into the applicability of the suspension mechanism is conducted.

As expected, the results showed that the overall PoS of suspension mechanism (PoS of upper component layer x PoS of bolts x PoS of sliding of roof bolts) is only 52 per cent (see Figure 7-24 for the distribution of safety factors in suspension mechanism). In other words, 48 per cent of the roof supported using the suspension mechanism with 1.2 m roof bolts will result in failure.

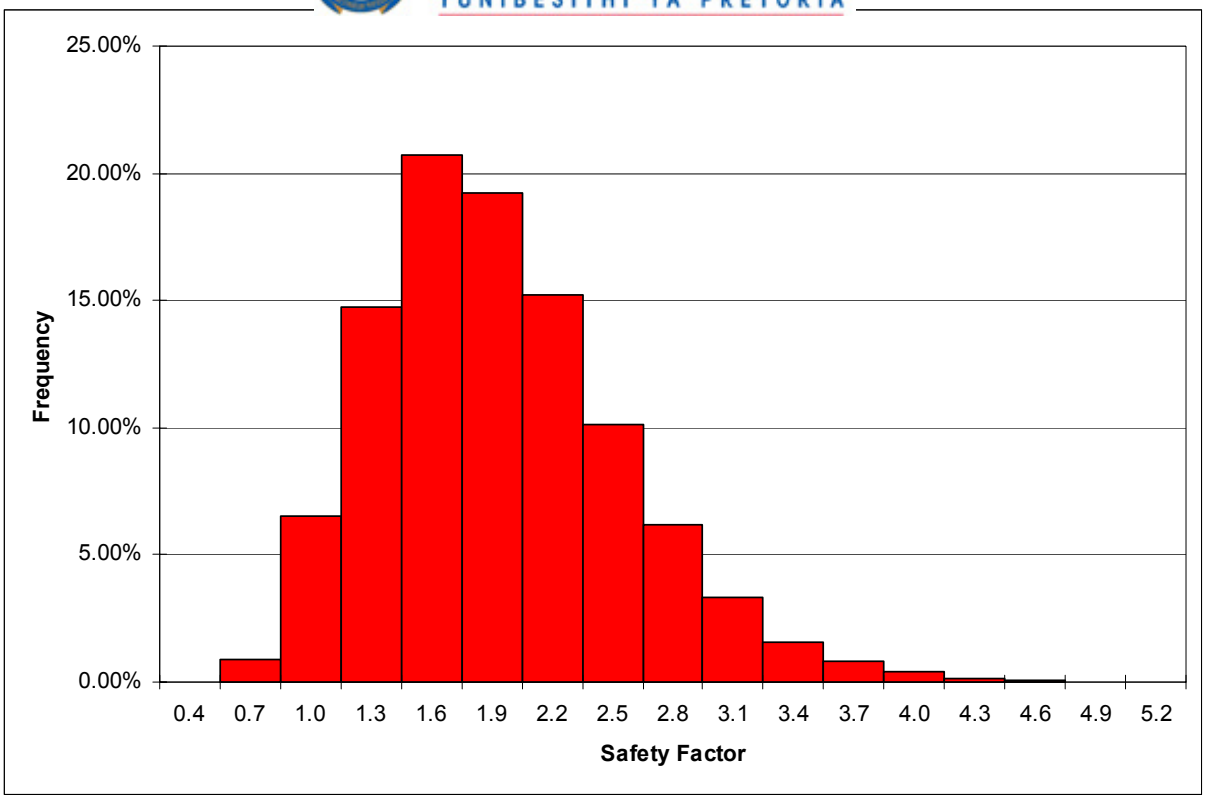

Figure 7-23 Distribution of safety factors of upper coal layer in suspension mechanism

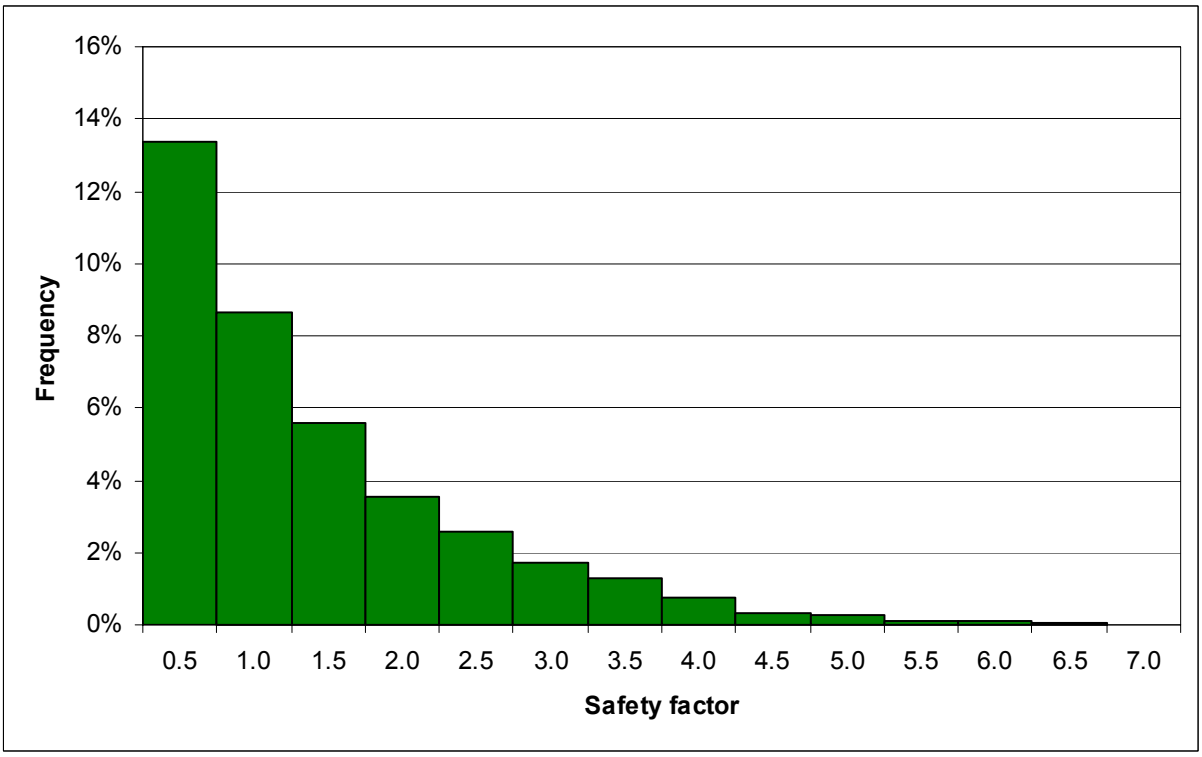

Figure 7-24 Distribution of safety factors in suspension mechanism using 1.2 m long roof bolts

Figure 7-25 shows the probability of stabilities and the reliability indexes for different lengths of roof bolts in suspension mechanism. As can be seen from this Figure that the maximum PoS that can be achieved is 92 per cent using 2.0 m long roof bolts, which does not meet the design criteria given in Table 7-4. Note that since the PoS of the suspension mechanism is dependent on the PoS of the upper coal layer, the maximum PoS that can be achieved for suspension mechanism is limited to 92.6 per cent.

From these analyses it is evident that the suspension mechanism, as it is currently used by the mine, is not the correct support mechanism for the roof conditions present at the mine. Therefore, beam building mechanism is recommended and a further study into the design of roof bolting system using the beam building mechanism is conducted.

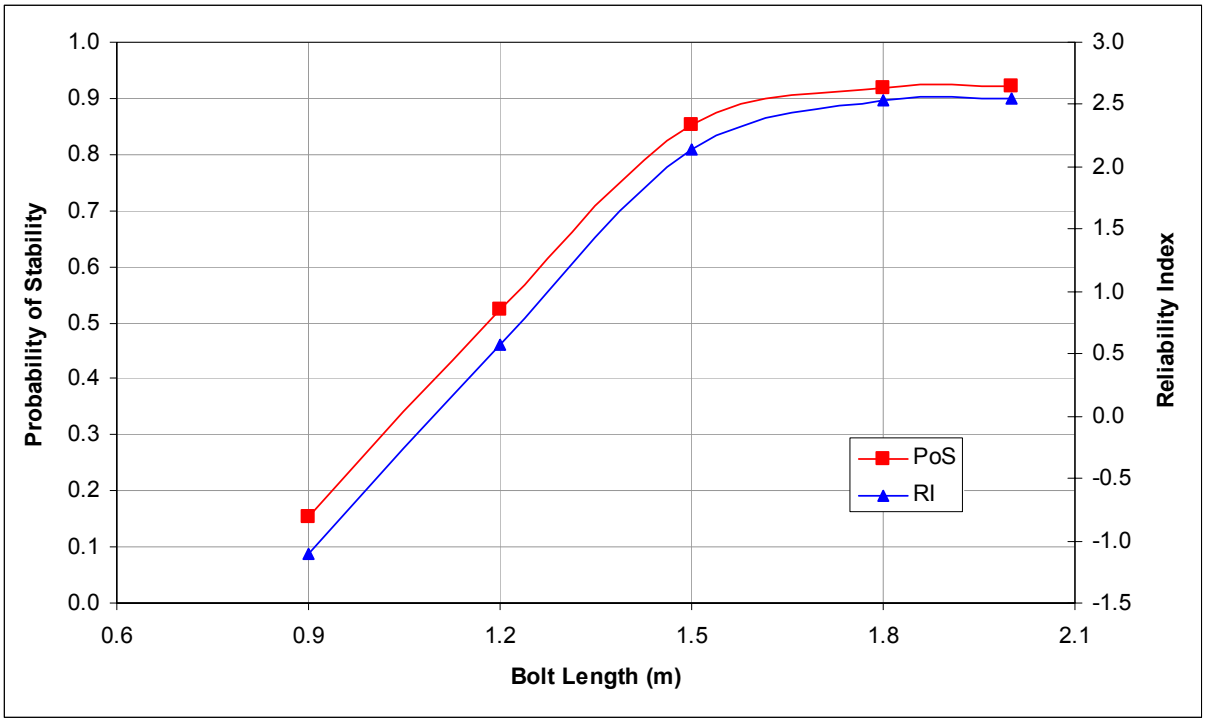

Figure 7-25 PoS and Reliability Index for suspension mechanisms for different roof bolt lengths

As a preliminary study, the mine's current support pattern, three bolts in a row with 2.0 m spacing was evaluated in beam building mechanism by assuming that the bolts are full-column. The probability of stabilities and the reliability indexes for different roof bolts lengths achieved from this study is presented in Figure 7-26. From this Figure it is evident that the current pattern used by the mine is not sufficient to achieve the required probability of stabilities even the bolts are full-column. Note that the overall probability of stabilities are presented in Figure 7-26 include probability of stability of shear loading, probability of bolt sliding and probability of bolt tension failures.

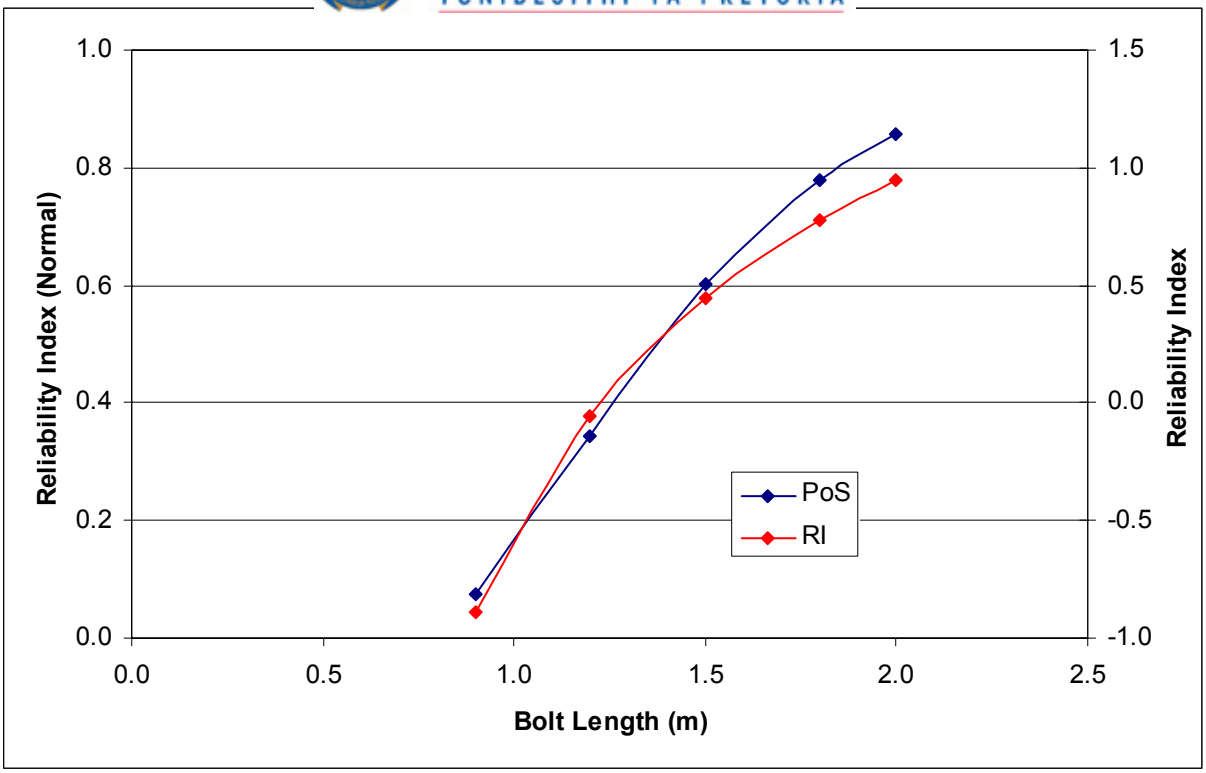

Figure 7-26 Probability of stability and reliability index of different length roof bolts, 3 roof bolts in a row

Table 7-9 shows the probability of stabilities and the reliability indexes achieved for 16 mm 4 and 5 roof bolt patterns using 2.0 m and 1.5 m row spacing. From this Table, the following *minimum* support patterns are recommended for different risk category areas:

- In moderately risk category areas:
  - four 1.8 m long roof bolts, 2.0 m row spacing
  - five 1.5 m long roof bolts, 2.0 m row spacing

- In serious risk category areas:
  - five 1.8 m long roof bolts, 2.0 m row spacing
  - four 1.5 m long roof bolts, 1.5 m row spacing

- In very serious risk category areas:
  - five 1.5 m long roof bolts, 1.5 m row spacing

Table 7-9 Stability analyses of different support patterns

Support pattern		Bolt Length (m)				
		0.9 m	1.2 m	1.5 m	1.8 m	2.0 m
4 bolts in a row 2.0 m spacing between the rows	Probability of stability	0.113	0.642	0.907	0.981	0.994
	Reliability Index	-0.834	0.461	1.238	1.756	2.015
5 bolts in a row 2.0 m spacing between the rows	Probability of stability	0.348	0.895	0.989	0.999	1.000
	Reliability Index	0.203	1.233	1.852	2.264	2.470
4 bolts in a row 1.5 m spacing between the rows	Probability of stability	0.435	0.959	0.999	1.000	1.000
	Reliability Index	0.498	1.784	2.556	3.070	3.328
5 bolts in a row 1.5 m spacing between the rows	Probability of stability	0.644	0.990	1.000	1.000	1.000
	Reliability Index	1.549	2.594	3.222	3.640	3.849

An important consideration at this stage is to conduct a simple cost analysis for different roof bolt systems to determine the financial viability of each system.

Once the bolting system is chosen and implemented, it is suggested that the support system should continuously be monitored and appropriate quality control procedures should be implemented (see Chapter 6.0 for details of quality control procedures).

As presented in Chapter 5, proactive rating systems (section performance and risk ratings) are effective in identifying support/roof performances. Therefore, detailed section performance and risk rating systems are also recommended in identifying the changing conditions, which may impact the support and the roof performances.

7.9 Conclusions

The ultimate aim of this Chapter was to develop a roof support design methodology that takes into account all natural variations exist within the rock mass and the mining process. This was achieved by adapting a probabilistic design approach using the well established stochastic modelling technique, which is widely used in civil and other engineering disciplines.

In the literature, it has been highlighted that one of the disadvantage of the probabilistic approach is the assumptions regarding the distribution functions. Using the data obtained throughout this thesis, the probability distributions of various input parameters have been established using the Anderson-Darling goodness of fit tests.

It is shown in this Chapter that the traditional deterministic roof bolt design methodologies provide some insight into the underlying mechanisms, but they are not well-suited to making predictions to roof support decision-making, as they cannot quantitatively address the risks and uncertainties that are inherently present.

An analysis of the data presented in Chapters 3 and 4 highlighted that for a 40 per cent increase in the span, taken across the diagonal of an intersection, relative to the roadway span, the magnitude of the displacement in the roof increased by a factor of four. The results also showed no evidence of a substantial increase in the height of the bed separated, potentially unstable roof strata, as is the case in the high horizontal stress driven beam buckling mechanism experienced in overseas coal mines. Analysis of the underground monitoring data also revealed that there is a good correlation between the underground measurements and simple beam theory, which has been used in the design of roof support systems for many years in South Africa. Therefore, in the development of the probabilistic approach, the deterministic approaches used in South Africa have been evaluated and improvements have been made, especially in the beam building mechanism.

Underground measurement data also showed that the maximum height of roof-softening measured in 54 sites in South African collieries is 2.5 m, which correlates well with the fall of ground data collected over 30 years in South Africa. The average height of roof-softening measured in these sites was 1.07 m.

The design approach established in this Chapter was applied to a well-defined case study in a colliery in the Witbank Coalfield, where the variations of all parameters that impact the roof and support behaviours were evident. Suspension mechanism has been used in this mine, which resulted in numerous roof falls. It has been shown using the input parameters collected from this mine that the suspension mechanism is not suitable for the conditions present. Therefore, the beam building mechanism was recommended for different risk category areas using four or five roof bolts with different lengths and row spacings.